Chemosphere 361 (2024) 142355

Contents lists available at ScienceDirect

Chemosphere

journal homepage: www.elsevier.com/locate/chemosphere

Continuous UV-C/H_2O_2 and UV-C/Chlorine applied to municipal secondary effluent and nanofiltration retentate: Removal of contaminants of emerging concern, ecotoxicity, and reuse potential

Fernando Rodrigues-Silva [a], Carla S. Santos [b,c], Joaquín A. Marrero [c,d], Rosa Montes [e], José Benito Quintana [e], Rosario Rodil [e], Olga C. Nunes [c,d], Maria Clara V.M. Starling [a], Camila C. Amorim [a,***], Ana I. Gomes [b,c,*], Vítor J.P. Vilar [b,c,**]

[a] Research Group on Environmental Applications of Advanced Oxidation Processes (GruPOA), Department of Sanitary and Environmental Engineering, The Federal University of Minas Gerais, Av. Antônio Carlos, 6627, 31270-901, Belo Horizonte, Minas Gerais, Brazil
[b] Laboratory of Separation and Reaction Engineering-Laboratory of Catalysis and Materials (LSRE-LCM), Faculty of Engineering University of Porto, Rua Dr. Roberto Frias, 4200-465, Porto, Portugal
[c] Associate Laboratory in Chemical Engineering (ALiCE), Faculty of Engineering, University of Porto, Rua Dr. Roberto Frias, 4200-465, Porto, Portugal
[d] Laboratory for Process and Reaction Engineering, Environment, Biotechnology and Energy (LEPABE), Faculdade de Engenharia, Universidade do Porto, Rua Dr. Roberto Frias, 4200-465, Porto, Portugal
[e] Aquatic One Health Research Center (ARCUS) & Department of Analytical Chemistry, Nutrition and Food Chemistry. R. Constantino Candeira S/N, IIAA building. Universidade de Santiago de Compostela, 15782, Santiago de Compostela, Spain

HIGHLIGHTS

- Photo-treatments applied to real municipal secondary effluent and its NF retentate.
- UV-C/H_2O_2 and UV-C/Chlorine were compared for the removal of CECs and ecotoxicity.
- UV-C/H_2O_2 removed 74% of average CECs and eliminated toxicity in secondary effluent.
- UV-C/AOPs removed 40% of average CECs in NF retentate posing challenges to AOPs.
- 1 mg L^{-1} of chlorine in NF permeate ensured *E.coli* <1 CFU/100 mL after 3-day storage.

GRAPHICAL ABSTRACT

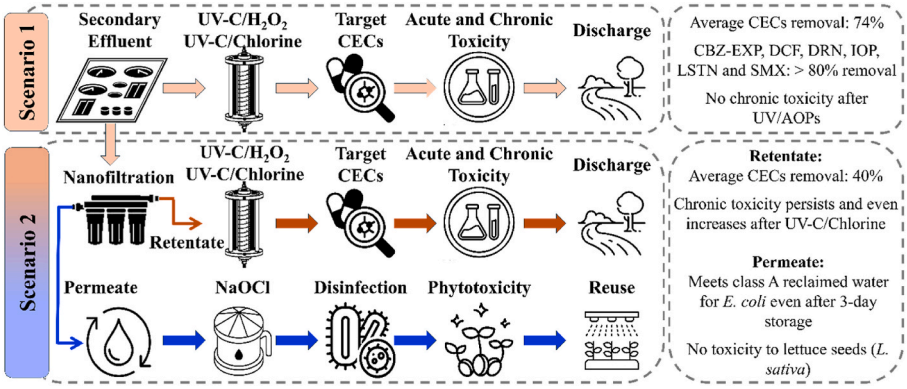

* Corresponding author. Associate Laboratory in Chemical Engineering (ALiCE), Faculty of Engineering, University of Porto, Rua Dr. Roberto Frias, 4200-465, Porto, Portugal.
** Corresponding author. Laboratory of Separation and Reaction Engineering-Laboratory of Catalysis and Materials (LSRE-LCM), Faculty of Engineering University of Porto, Rua Dr. Roberto Frias, 4200-465, Porto, Portugal.
*** Corresponding author.
E-mail addresses: camila@desa.ufmg.br (C.C. Amorim), ana.isabelgomes@fe.up.pt (A.I. Gomes), vilar@fe.up.pt (V.J.P. Vilar).

https://doi.org/10.1016/j.chemosphere.2024.142355
Received 7 February 2024; Received in revised form 14 May 2024; Accepted 15 May 2024
Available online 18 May 2024

ARTICLE INFO

Handling editor: Xiangru Zhang

Keywords:
Environmental sustainability
Membrane separation
Reclaimed water
Safe wastewater discharge
UV-Driven advanced oxidation processes

ABSTRACT

As global effects of water scarcity raise concerns and environmental regulations evolve, contemporary wastewater treatment plants (WWTPs) face the challenge of effectively removing a diverse range of contaminants of emerging concern (CECs) from municipal effluents. This study focuses on the assessment of advanced oxidation processes (AOPs), specifically UV-C/H_2O_2 and UV-C/Chlorine, for the removal of 14 target CECs in municipal secondary effluent (MSE, spiked with 10 μg L^{-1} of each CEC) or in the subsequent MSE nanofiltration retentate (NF_R, no spiking). Phototreatments were carried out in continuous mode operation, with a hydraulic retention time of 3.4 min, using a tube-in-tube membrane photoreactor. For both wastewater matrices, UV-C photolysis (3.3 kJ L^{-1}) exhibited high efficacy in removing CECs susceptible to photolysis, although lower treatment performance was observed for NF_R. In MSE, adding 10 mg L^{-1} of H_2O_2 or Cl_2 enhanced treatment efficiency, with UV-C/H_2O_2 outperforming UV-C/Chlorine. Both UV-C/AOPs eliminated the chronic toxicity of MSE toward *Chlorella vulgaris*. In the NF_R, not only was the degradation of target CECs diminished, but chronic toxicity to *C. vulgaris* persisted after both UV-C/AOPs, with UV-C/Chlorine increasing toxicity due to potential toxic by-products. Nanofiltration permeate (NF_P) exhibited low CECs and microbial content. A single chlorine addition effectively controlled *Escherichia coli* regrowth for 3 days, proving NF_P potential for safe reuse in crop irrigation (<1 CFU/100 mL for *E. coli*; <1 mg L^{-1} for free chlorine). These findings provide valuable insights into the applications and limitations of UV-C/H_2O_2 and UV-C/Chlorine for distinct wastewater treatment scenarios.

1. Introduction

Contaminants of emerging concern (CECs) pose a great challenge to environmental integrity and public health, encompassing a diverse range of pollutants such as endocrine-disrupting substances (Kasonga et al., 2021), pharmaceuticals and personal care products (Sengar and Vijayanandan, 2022), persistent organic pollutants (Vasseghian et al., 2021), antibiotic-resistant bacteria and genes (Starling et al., 2021), among others. Typically, urban wastewater treatment in WWTPs involves two stages: primary sedimentation and secondary biological oxidation (commonly conventional activated sludge, CAS). As a result, CECs continue to be discharged into the environment, exerting adverse effects on aquatic ecosystems, and potentially impacting human health. Pistocchi et al. (2022) highlighted the urgency of addressing this issue, showing that CECs discharged after secondary treatment may result in cumulative toxicity equivalent to discharging 30% of total wastewater generated in the European Union without any treatment. Thus, the effectiveness of conventional two-stage treatment is insufficient for water reuse, with several CECs still detected in secondary effluents (Krzeminski et al., 2019; Sá et al., 2022). Nevertheless, treated wastewater holds promise as a continuous source of high-quality water to meet future water needs, especially for agricultural purposes. However, if not treated properly, wastewater reuse can pose risks to public health and the environment, given the potential presence of toxic chemicals and pathogenic microorganisms (Verlicchi et al., 2023). To address these concerns, the European Union (EU) has adopted the EU Regulation on minimum requirements for water reuse (EURegulation_2020/741, 2020). Furthermore, the EU has proposed a new Urban Wastewater Treatment Directive (EU-UWWTD, 2022), targeting new standards and limit values, and obligations for large wastewater treatment plants (WWTPs) to reduce by 80% a specified set of CECs. Therefore, advanced treatment technologies – such as advanced oxidation (AOPs) and membrane filtration processes – are in focus as a subsequent treatment stage.

UV-driven AOPs, traditionally relying on the generation of highly reactive and non-selective hydroxyl radicals ($HO^{\bullet}$), offer several advantages, namely (i) do not transfer the pollutants into another phase, such as in physical (separation) processes, (ii) are effective in disinfecting pathogenic microorganisms that might be present in the wastewater, and (iii) have fast reaction rates for a wide range of contaminants (Khajouei et al., 2022). Among UV-AOPs, UV-C/H_2O_2 stands out as the most established technology for wastewater treatment (Farzanehsa et al., 2023). Recently, the UV-C/Chlorine process has emerged as an alternative to UV-C/H_2O_2 in removing CECs (Farzanehsa et al., 2023; Guo et al., 2018; Khajouei et al., 2022). Beyond the generation of $HO^{\bullet}$, UV-C/Chlorine also produces different selective reactive chlorine species (RCS, such as $Cl^{\bullet}$, $ClO^{\bullet}$, and $Cl_2^{\bullet-}$). Furthermore, compared to UV-C/H_2O_2, aqueous chlorine presents a higher UV molar absorption coefficient (ε) and quantum yield (Φ) ($\varepsilon_{HOCl,254nm} = 59\ M^{-1}\ cm^{-1}$, $\varepsilon_{OCl\text{-},254nm} = 66\ M^{-1}\ cm^{-1}$, and $\Phi_{HOCl,254nm} = 1.0\ M\ E^{-1}$, $\Phi_{OCl\text{-},254nm} = 0.6\ M\ E^{-1}$ (Feng et al., 2007) *vs* $\varepsilon_{H2O2,254nm} = 19\ M^{-1}\ cm^{-1}$ and $\Phi_{H2O2,\ 254nm} = 0.5\ mol\ E^{-1}$ (Baxendale and Wilson, 1957)). Therefore, UV-C/Chlorine will likely produce more radicals in the reaction bulk than UV-C/H_2O_2 (Ike et al., 2019; Khajouei et al., 2022).

Adopting UV-AOPs in large-scale facilities faces challenges due to prolonged treatment times and costs. To address this, novel technological approaches are actively under investigation. Vilar et al. (2020) proposed the tube-in-tube membrane photoreactor, which demonstrated efficient degradation of a variety of CECs in real secondary effluents. This occurred within short treatment times (few minutes) using different UV-AOPs, including UV/TiO_2/H_2O_2 (Castellanos et al., 2020), UV/TiO_2/$S_2O_8^{2-}$ (Lumbaque et al., 2021), UV/Ag_2MoO_4/H_2O_2 and UV/Ag_2MoO_4/$S_2O_8^{2-}$ (Vazquez et al., 2023), and photo-Fenton under natural pH conditions (Díaz-Angulo et al., 2021; Santos et al., 2023). This annular photoreactor, featuring tangential inlet and outlet tubes, promotes a helical flow of water around the central membrane, potentiating a high degree of mixing even under a low Reynolds number (Espíndola and Vilar, 2020; Peres et al., 2015). Simultaneously, the selected oxidant (or iron-catalyst solution, in the photo-Fenton case) is continuously delivered through the membrane pores, acting as multiple dosing points throughout the photoreactor, into the annular reaction zone. Combining these features contributes to a more homogeneous radial and axial oxidant distribution along the tubular photoreactor length (Castellanos et al., 2020; Vilar et al., 2020).

In another treatment scenario foreseeing water reuse, membrane processes like nanofiltration (NF) applied downstream of a biological process have proven potential to act as a pathogen and CEC barrier (Krzeminski et al., 2019; Schwermer et al., 2018). A disinfection step is then needed for the NF permeate to prevent possible microbial regrowth and biofilm formation in the distribution system for reclaimed water (Wang et al., 2022). Sodium hypochlorite (NaClO) is widely used in WWTPs (the cheapest option), but the toxicity of by-products and residual chlorine must be considered (Rizzo et al., 2020). Yet, there is still a need to treat the NF retentate, typically concentrated by a factor of 3–6. An opportunity arises to apply AOPs since pollutants are oxidized more effectively as their initial concentration increases (Miralles-Cuevas et al., 2016). However, their application to NF retentate is still scarce and demands further study.

Motivated by the existing challenges in wastewater treatment and the need for more effective solutions, our study aims to investigate the application of a UV-AOPs stage, UV-C/H_2O_2 and UV-C/Chlorine, addressing two distinct treatment approaches. In scenario 1, UV-AOP

Table 1
Selected contaminants of emerging concern (CECs).

Category	Contaminant	Acronym	Chemical composition	$\varepsilon_{254,app}$ [a] (M^{-1} cm^{-1})	$\Phi_{254,app}$ [a] (mol E^{-1})	$k_{HO\bullet}$ [b] ($M^{-1}s^{-1}$)	$k_{Cl\bullet}$ [c] (M^{-1} s^{-1})	$k_{Cl2\bullet-}$ [c] (M^{-1} s^{-1})	$k_{ClO\bullet}$ [c] (M^{-1} s^{-1})
Beta-blocking agents	Atenolol	ATNL	$C_{14}H_{22}N_2O_3$	5.3×10^2	3.6×10^{-2}	8×10^9	2.3×10^{10}	4.1×10^8	8.7×10^7
	Bisoprolol	BSPL	$C_{18}H_{31}NO_4$	–	–	Unknown			
Carbamazepine and Metabolites	Carbamazepine	CBZ	$C_{15}H_{12}N_2O$	6.1×10^3	6×10^{-4}	8.8×10^9	5.6×10^{10}	$<0.5 \times 10^8$	2.0×10^8
	10.11 Carbamazepine-epoxide	CBZ-EPX	$C_{15}H_{12}N_2O_2$	–	–	Unknown			
Anti-Inflammatory Drugs	Diclofenac	DCF	$C_{14}H_{10}Cl_2NNaO_2$	6.8×10^3	2.3×10^{-1}	7.5×10^9	3.8×10^{10}	1.2×10^9	3.5×10^8
Insect Repellents	N,N-diethyl-*meta*-toluamide	DEET	$C_{12}H_{17}NO$	–	–	5×10^9	3.8×10^9		
Herbicides	Diuron	DRN	$C_9H_{10}Cl_2N_2O$	1.6×10^4	1.9×10^{-2}	6.6×10^9			
X-Ray Contrast Agent	Iopromide	IOP	$C_{18}H_{24}I_3N_3O_8$	2.2×10^4	3.9×10^{-2}	3.3×10^9	2.8×10^{10}	2.1×10^9	
Fire Retardants	Melamine	MLN	$C_3H_6N_6$	–	–	1×10^4			
Angiotensin II Receptor Blockers	Irbesartan	ISTN	$C_{25}H_{28}N_6O$	–	–	1×10^{10}			
	Losartan	LSTN	$C_{22}H_{22}ClKN_6O$	1.2×10^4	1.3×10^{-2}	Unknown			
	Valsartan	VSTN	$C_{24}H_{29}N_5O_3$	–	–	1×10^{10}			
Antibiotic	Sulfamethoxazole	SMX	$C_{10}H_{11}N_3O_3S$	1.7×10^4	3.0×10^{-2}	5.5×10^9	3.6×10^9	4.7×10^8	$<2.2 \times 10^9$
Psychiatric Drugs	Venlafaxine	VLX	$C_{17}H_{27}NO_2$	3.8×10^2	9.7×10^{-2}	8.8×10^9		3.6×10^8	1.7×10^8

[a] Values for molar extinction coefficient (ε_{254nm}) and quantum yield (Φ_{254nm}) were obtained from Salgado et al. (2013), Wols et al. (2015), Baeza and Knappe (2011).
[b] Kinetic constants for the reaction with HO•($k_{HO\bullet}$) were obtained from Wols et al. (2013), Baeza and Knappe (2011), Huber et al. (2003), Guo et al. (2019).
[c] Kinetic constants for the reaction with chlorine radicals ($k_{Cl\bullet}$, $k_{Cl2\bullet-}$, $k_{ClO\bullet}$) were obtained from Lei et al. (2019), Guo et al. (2018), Lei et al. (2021), Sun et al. (2016), Allard et al. (2016).

is applied to municipal secondary effluent (MSE), while in scenario 2, MSE is subject to an NF stage and the UV-AOP is applied to the subsequent NF retentate (NF_R). For both treatment scenarios, the UV-C photolysis, UV-C/H_2O_2, and UV-C/Chlorine tests were conducted in continuous mode, with a residence time of 3.4 min, using the tube-in-tube membrane photoreactor. The efficiency of photo-treatments in removing several target CECs, belonging to different contaminant groups, was assessed and compared. The selected CECs are all classified as (very-)Persistent/(very-)Mobile/(potentially-)Toxic (according to Montes et al. (2022) and Verlicchi et al. (2023)) and include four compounds (carbamazepine (CBZ), diclofenac (DCF), irbesartan (ISTN), and venlafaxine (VLX)) listed in the EU-UWWTD proposal (EU-UWWTD, 2022). Given the potential for reuse in agricultural irrigation, the levels of contamination by *Escherichia coli* (*E. coli*) were evaluated for the nanofiltration permeate (NF_P). The potential for *E. coli* regrowth after disinfection with NaOCl was also verified. To comprehensively evaluate the potential impacts of treatment processes, bioassays were made to assess the potential toxicity for various trophic levels (decomposer and producers), encompassing both aquatic and terrestrial organisms (bioluminescent bacteria *Aliivibrio fischeri*, the green algae *Chlorella vulgaris*, and seeds of *Lactuca sativa*).

2. Materials and methods

2.1. Chemicals

The target CECs used in this research are listed in Table 1 and further details are provided in the Supplementary File (Table SM-1). Stock solutions of CECs were prepared for spiking to the MSE matrix, either in methanol or ultrapure water, according to the solubility of the compounds. CECs were provided by Sigma-Aldrich, TCI, AlfaAesar, and ACROS Organics (purity >95 %). The addition of CECs dissolved in methanol had a contribution of ~4 mg C L^{-1} to the organic carbon content of the MSE matrix. NaClO (VWR, 14% active chlorine) and H_2O_2 (Labkem, 30% (v/v)) were used as oxidants. Sodium bisulfite (Na_2SO_3) (VWR) or catalase from bovine liver (Sigma-Aldrich) were added to stop the oxidizing capacity of NaClO and H_2O_2, respectively. Metavanadate and *N,N*-Diethyl-*p*-phenylenediamine (DPD) sulfate pentahydrate were purchased from Sigma-Aldrich (purity >98%).

2.2. Analytical determinations

Samples were characterized for temperature and pH (portable pHmeter Hanna Instruments, HI8424), electrical conductivity (Hanna Instruments, Edge HI2003-02), chemical oxygen demand (COD, 5220 D (APHA, 2017)), total suspended solids (TSS, 2540 E (APHA, 2017)) and turbidity (HANNA HI 88703 turbidity meter). Free and the total chlorine concentrations were determined according to the DPD colorimetric method (4500-Cl G (APHA, 2017)). H_2O_2 quantification was performed using ammonium metavanadate, according to Nogueira et al. (2005). UV–Vis measurements were performed on UV–Vis equipment (Spectroquant, Prove 600). Dissolved organic carbon (DOC) and dissolved inorganic carbon (DIC) were quantified in a total organic carbon (TOC) analyzer (Shimadzu, TOC-VCSN). The concentration of anions was analyzed by ion chromatography (Dionex, ICS-2100 LC) equipped with an IonPac column (AS11-HC, 250 mm × 4 mm) and an anion self-regenerating suppressor (ASRS® 300, 4 mm), while cations (Dionex, DX-120 LC) were also determined with an IonPac column (CS12A, 250 mm × 4 mm) at ambient temperature and a cation self-regenerating (CSRS Ultra II, 4 mm).

2.3. Water matrices

The water matrices submitted to treatment in this study - municipal secondary effluent (MSE), and the retentate (NF_R) and permeate (NF_P) resulting from a subsequent NF stage - were collected on different days

Table 2
Physicochemical characteristics and native concentrations of target CECs for municipal secondary effluent (MSE), nanofiltration retentate (NF_R) and permeate (NF_P) used in this study, and concentration ranges (minimum and maximum values) found for MSE collected in the same WWTP.

Parameters (units)	Typical MSE[a] (min - max)	MSE	NF_R	NF_P
Dissolved Organic Carbon (mg L^{-1})	13–30	23	51	0.9
Dissolved Inorganic Carbon (mg L^{-1})	30–77	39	65	42
Chemical Oxygen Demand (mg L^{-1})	21–80	74	206	1.2
Total Suspended Solids (mg L^{-1})	4–36	14	9	2
Turbidity (NTU)	1–16	3.1	1.7	0.1
Absorbance UV_{254} (cm^{-1})	0.14–0.35	0.23	1.2	0.004
Phosphates (PO_4^{3-}) (mg L^{-1})	4–26	5	79	2
Sulfates (SO_4^{2-}) (mg L^{-1})	37–339	43	636	2
Nitrites (NO_2^-) (mg L^{-1})	<1–8	2	27	<LQ
Chlorides (Cl^-) (mg L^{-1})	83–308	130	561	121
Nitrates (NO_3^-) (mg L^{-1})	<1–26	13	135	<LQ
Sodium (Na^+) (mg L^{-1})	100–133	112	751	99
Ammonium (NH_4^+) (mg L^{-1})	1–78	14	57	10
Potassium (K^+) (mg L^{-1})	24–31	18	111	16
Magnesium (Mg^{2+}) (mg L^{-1})	5–9	8	44	3
Calcium (Ca^{2+}) (mg L^{-1})	28–34	31	224	10
Conductivity (μS cm^{-1})	202–1519	846	2204	610
pH	7.1–7.6	7.7	8.1	7.6
ATNL (ng L^{-1})	< LQ – 425	< LQ	< LQ	< LQ
BSPL (ng L^{-1})	168–585	158	1485	< LQ
CBZ (ng L^{-1})	40–888	242	2953	< LQ
CBZ-EPX (ng L^{-1})	106–519	45	4994	< LQ
DCF (ng L^{-1})	364–3164	506	9564	< LQ
DEET (ng L^{-1})	109–1062	127	< LQ	< LQ
DRN (ng L^{-1})	< LQ – 200	< LQ	185	< LQ
IOP (ng L^{-1})	< LQ - 4680	3432	21209	< LQ
ISTN (ng L^{-1})	951–2426	875	3886	< LQ
LSTN (ng L^{-1})	< LQ	< LQ	1768	< LQ
VSTN (ng L^{-1})	< LQ - 1480	843	< LQ	< LQ
SMX (ng L^{-1})	309–1021	136	4142	< LQ
VLX (ng L^{-1})	292–1064	291	2036	< LQ
MLN (ng L^{-1})	< LQ - 4440	1078	12335	692

[a] Values collected from previous works carried out with MSE from the same WWTP as this study (Castellanos et al., 2020; Diório et al., 2021; Lumbaque et al., 2020; Montes et al., 2022; Presumido et al., 2023; Santos et al., 2023; Vazquez et al., 2023).

in December 2022 and January 2023. The MSE was sampled at the outlet of the secondary settling tank of a municipal WWTP (population equivalent of 150 000) located in the North of Portugal. A pilot-scale NF membrane system (Aquaquímica Ltda., RO-250; Lenntech, NE 4040-70) was implemented at the same municipal WWTP. The wastewater fed into the NF system was collected at the outlet of the secondary clarifier, stored in a tank (1 m^3 capacity), and pumped into the membrane unit. The pump (EFAFLU, BMV 2–18) can operate with pressures of 7–15 bar and a maximum permeate flow of 250 L h^{-1}. The NF_R was recirculated back to the feed tank until reaching a final volume of 375 L (volumetric concentration factor ≈ 2.7), while the NF_P was continuously discharged. To minimize suspended solids, the NF_R was pumped through a sand filtration system before sampling. Table 2 shows the main physico-chemical characteristics of each matrix, including native concentrations of CECs.

2.4. Experimental setup and procedure

2.4.1. Photo-oxidation treatment tests: municipal secondary effluent and nanofiltration retentate

Photo-oxidation tests were performed in a lab-scale tube-in-tube photoreactor (Fig. 1) consisting of an inner ultrafiltration membrane (ceramic, γ-Al_2O_3 membrane; pore size 10 nm; $Ø_{external}$ 2.0 cm; $Ø_{internal}$ 1.6 cm; illuminated length 17.4 cm) and an outer quartz tube ($Ø_{external}$ 4.2 cm; $Ø_{internal}$ 3.8 cm; illuminated length 17.4 cm), sealed by mobile polypropylene flanges. Distributed externally and equidistant to the quartz tube, four low-pressure UV-C lamps (TUV 11W FAM/10X2SBOX, λ of 254 nm) are used as a light source. The experimental installation is surrounded by a square aluminum reflector covered with aluminum foil (photon flow of 2.3 ± 0.2 W, determined by ferrioxalate actinometry). The MSE or NF_R was pumped continuously through the annular reaction zone (ARZ) with partial recirculation of the outlet stream.

All treatment tests were carried out at the natural pH of the matrices and, in the case of MSE with the prior addition of the 14 target CECs (at 10 μg L^{-1} for each). After spiking the MSE matrix, the native molar concentration for each CEC contributed ≤10% to the final molar concentration, except for IOP (34%). Experiments with NF_R were not spiked with CECs. For both matrices, feed and recirculation flows were set to 2.5 L h^{-1} and 27.5 L h^{-1}, respectively, corresponding to a residence time (RT) of 3.4 min. Stock solutions of H_2O_2 (735 mM, pH = 4.3) or NaClO (486 mM; pH = 11.8) were injected through the lumen side of the membrane using a syringe pump (Chemyx Inc., Nexus 6000). Experiments were performed testing three concentrations of each oxidant in the ARZ. For MSE, the oxidant concentrations were 5, 10, and 20 mg L^{-1} (as H_2O_2 and Cl_2). These concentrations were selected based on the typical chlorine concentration applied in the disinfection process of treatment plants (Cerreta et al., 2019). Considering the higher in (organic) matter content in the NF_R matrix, the treatment approach was to increase these concentrations 4-fold (20, 40, and 80 mg L^{-1}). Three samples were withdrawn from the reactor outlet under steady-state conditions for analysis and characterization. The main experimental conditions are summarized in Table 3.

2.4.2. Residual disinfection tests: nanofiltration permeate

NF_P stream was collected in 1 L sterile glass beakers and the desired dose of NaOCl (0, 1, and 3 mg Cl_2 L^{-1}) was added to the respective beaker. Samples were withdrawn in sterile beakers after 30 min of contact (initial sample) and after 3 days (final sample) for *Escherichia coli* enumeration and free residual chlorine measurement. *E. coli* was selected as an indicator organism for residual disinfection efficiency since it is a quality requirement for reclaimed water for agricultural irrigation (EURegulation_2020/741, 2020).

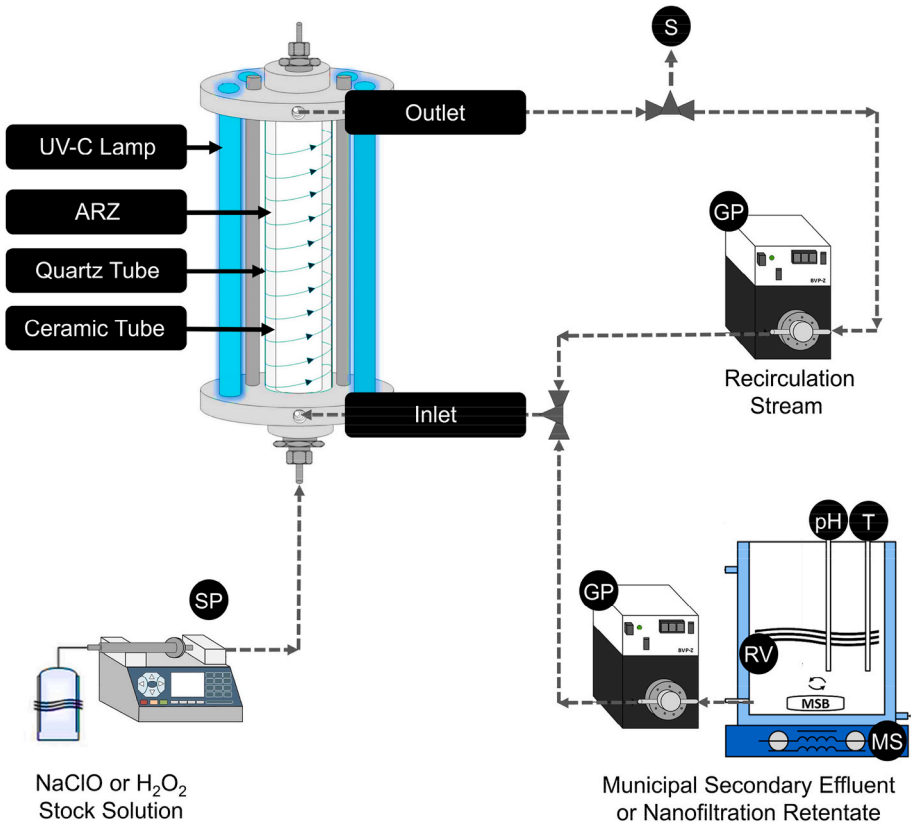

Fig. 1. Simplified schematic representation of the tube-in-tube membrane photoreactor setup. Legend: ARZ – Annular Reaction Zone; GP – Gear Pump; MS – Magnetic Stirrer; MSB – Magnetic Stir Bar; pH – pH Sensor; RV – Recirculatory Vessel; S – Sampling; SP – Syringe Pump; T – Temperature Sensor.

Table 3
- Experimental conditions and response variables assessed for the tests carried out with MSE, NF_R and NF_P.

#	Matrix	Radiation	Oxidant	$[Oxidant]_{ARZ}$ (mg L^{-1})	Response variables				
					CECs	AT	CT	PT	*E. coli*
1	MSE	UV-C	–	–	X	–	–	–	–
2	MSE	–	H_2O_2	20	X	–	–	–	–
3	MSE	–	NaClO	20	X	–	–	–	–
4	MSE	UV-C	H_2O_2	5	X	–	–	–	–
5	MSE	UV-C	H_2O_2	10	X	X	X	X	–
6	MSE	UV-C	H_2O_2	20	X	X	X	X	–
7	MSE	UV-C	NaClO	5	X	–	–	–	–
8	MSE	UV-C	NaClO	10	X	X	X	X	–
9	MSE	UV-C	NaClO	20	X	X	X	X	–
10	NF_R	UV-C	–	–	X	–	–	–	–
11	NF_R	–	H_2O_2	80	X	–	–	–	–
12	NF_R	–	NaClO	80	X	–	–	–	–
13	NF_R	UV-C	H_2O_2	20	X	–	–	–	–
14	NF_R	UV-C	H_2O_2	40	X	X	X	–	–
15	NF_R	UV-C	H_2O_2	80	X	X	X	–	–
16	NF_R	UV-C	NaClO	20	X	–	–	–	–
17	NF_R	UV-C	NaClO	40	X	X	X	–	–
18	NF_R	UV-C	NaClO	80	X	X	X	–	–
19	NF_P	–	–		–	–	–	X	X
20	NF_P	–	NaClO	1	–	–	–	X	X
21	NF_P	–	NaClO	3	–	–	–	X	X

Legend: MSE – municipal secondary effluent; NF_R – nanofiltration retentate; NF_P – nanofiltration permeate; ARZ – annular reaction zone; CEC – contaminant of emerging concern; AT – acute toxicity with *Aliivibrio fischeri*; CT – chronic toxicity with *Chlorella vulgaris*; PT – phytotoxicity with *Lactuca sativa.*

2.5. CECs analysis

For each treatment test, a sample from the reactor inlet and three samples collected from the reactor outlet at steady-state were analyzed for quantification of the 14 target CECs. The analytical determination of target CECs in the water samples was performed by direct injection on a liquid chromatography coupled to tandem mass spectrometry (LC-MS/MS) system; in this case, an Acquity UPLC® H class interfaced to a Xevo TQD triple quadrupole mass spectrometer (Waters, Milford, MA, USA). Further details on the methodology are described in the Supplementary File.

2.6. Ecotoxicity assessment

Samples were carefully collected in clean amber flasks and either immediately subjected to toxicity testing or preserved at −8 °C before assays. MSE sampled after treatments were analyzed for acute toxicity with *Aliivibrio fischeri* (decomposer), chronic toxicity with *Chlorella vulgaris* (producer), and phytotoxicity with *Lactuca sativa* (producer) seeds. The same assays were applied to NF_R, except for phytotoxicity. In turn, phytotoxicity assays were carried out for the NF_P due to the potential of this matrix to be used as reclaimed water for crop irrigation.

2.6.1. Acute toxicity bioassays

Acute toxicity was assessed by Microtox® (model LX, ModernWater) with the bioluminescent bacteria *Aliivibrio fischeri* (ISO, 2007). Results were expressed as the concentration that caused an acute effect (luminescence decay) to 50% of the population (EC_{50}) according to the statistical analysis performed in Microtox LX integrated software.

2.6.2. Chronic toxicity bioassays

Chronic toxicity was evaluated by the growth inhibition of the green algae *Chlorella vulgaris*, following the Organization for Economic Co-operation and Development Guidelines (OECD, 2011). *C. vulgaris* cells were incubated and withdrawn at different cultivation periods after reaching the exponential growth phase. Dry biomass weight was correlated to the optical density of microalgal suspensions at 680 nm (OD_{680}) (Porto et al., 2022). Then, algae were incubated with samples (non-diluted (100%) and under different dilution factors (DF): 50% - DF 2; 25% - DF 4; 12.5% - DF 8; 6.25% - DF 16; 3.12% - DF 32; and 1.56% - DF 64, in triplicates) for 72 h under axenic conditions. After 72 h, cell growth was determined by measuring OD_{680} and dry biomass. Data underwent homoscedasticity (F test, $p < 0.05$) and normality (Shapiro-Wilk test, $p < 0.05$) analyses. Subsequently, an analysis of variance (ANOVA, $p < 0.05$) was conducted to identify significant differences in biomass growth compared to the control. In addition, statistical analysis was performed according to the dose-response curve to determine EC_{50} values for the samples that resulted in toxic endpoints.

2.6.3. Phytotoxicity

Phytotoxicity was assessed by analyzing germination and root elongation of *Lactuca sativa* seeds as described elsewhere (Rodrigues-Silva et al., 2022). The Germination Index (GI) was calculated according to Equation (1), where NGS refers to the number of germinated seeds, and TNS is the total number of seeds (Garcia et al., 2009). The Relative Root Growth Index (RGI) was determined using Equation (2), where ARS represents the average root length for organisms exposed to samples, and ARC is the average root length observed for the control. The RGI results were categorized into three effect categories: inhibition ($0 < RGI < 0.8$), non-significant ($0.8 < RGI < 1.2$), and stimulation ($RGI > 1.2$).

$$GI\ (\%) = (NGS / TNS) \times 100 \quad (1)$$

$$RGI = ARS/ARC \quad (2)$$

2.7. Enumeration of Escherichia coli

The abundance of *Escherichia coli* was measured for the nanofiltration permeate samples using the membrane filtration method. A volume of 1, 10, or 100 mL for each sample was filtered (in triplicate) through cellulose nitrate membrane filters (0.22 μm porosity; Whatman, UK). Afterward, the filtering membranes were incubated on Chromogenic Coliform Agar (CCA, VWR Chemicals) at 37 °C for 24 h. The cultivable bacteria counts were expressed as the average of log colony forming units (CFU) per 100 mL.

3. Results and discussion

3.1. Scenario 1: UV-AOP applied to municipal secondary effluent

3.1.1. Municipal secondary effluent

The municipal secondary effluent (MSE), collected for the post-treatment tests carried out for scenario 1, exhibits physicochemical quality suitable for discharge into water compartments (chemical oxygen demand (COD) < 125 mg O_2 L^{-1} and total suspended solids (TSS) < 35 mg L^{-1}, according to Directive 91/271/EEC (1991)). Overall, the assessed physicochemical parameters fall within the typical range found for the MSE of this WWTP (Table 2). Of the 14 CECs investigated in this study, 11 were detected in the MSE matrix, with ATNL (β-blocker agent), CBZ-EPX (an active metabolite of carbamazepine), and DRN (herbicide) showing concentrations below the limit of quantification (LQ, see Table SM-3). In contrast, MLN (flame retardant) and IOP (X-ray contrast agent) exhibited the highest concentrations (1078 and 3432 ng L^{-1}, respectively). The observed CEC levels also align with the concentration ranges found in MSE from this WWTP, characterized by significant variability in contamination levels across various compounds (Table 2). The four CECs foreseen in the EU-UWWTD proposal (CBZ, DCF, ISTN, and VLX) were all detected in the MSE, as their elimination during conventional secondary treatment is not expected to be significant. However, some removal levels are known to occur, mainly due to the sorption of the CECs in activated sludge rather than biodegradation (Bessa et al., 2021; Paxéus, 2004).

3.1.2. Removal of CECs by UV-C photolysis

The degradation of the 14 target CECs was initially evaluated under

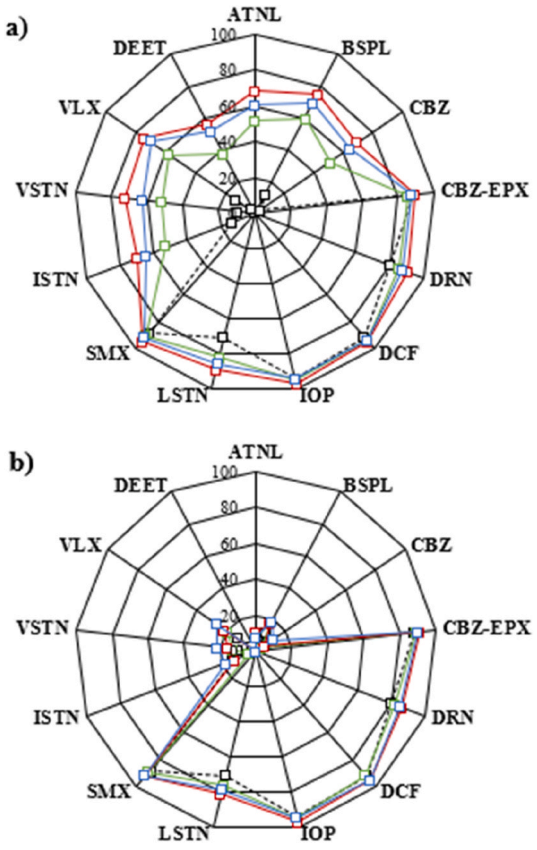

Fig. 2. Removal efficiencies (%) for the 14 target CECs spiked in MSE for UV-C photolysis (-□- test #1) and a) UV-C/H_2O_2 or b) UV-C/NaHOCl. Oxidant dose of 5 mg L^{-1} (-□-tests #4 and #7), 10 mg L^{-1} (-□- tests #5 and #8) and 20 mg L^{-1} (-□- tests #6 and #9). NOTE: MLN was not removed for any tested condition and is therefore not represented in the graphs.

UV-C radiation (3.3 kJ L^{-1}) without oxidant dosage (test #1) and in dark conditions with a continuous dosage of 20 mg L^{-1} of the selected oxidant, H_2O_2 (test #2) or NaOCl (test #3). Although NaClO and H_2O_2 were not effective in oxidizing the target CECs in the absence of UV-C radiation (removals <10% for all CECs), UV-C photolysis proved to be highly efficient in degrading six target CECs (CBZ-EXP, DCF, DRN, IOP, LSTN, and SMX), obtaining removals >70% (Figure SM-1). On the other hand, three target CECs (BSPL, ISTN, and VLX) had very modest removals (~13%), while the remaining five CECs showed negligible signs of degradation (<10% for ATNL, CBZ, DEET, MLN, and VSTN).

The breakdown of CECs under UV-C irradiation (λ = 254 nm) is governed by the absorption of photons by the target compounds, a process influenced by their respective molar extinction coefficient (ε_{254nm}) and quantum yield (Φ_{254nm}). The values outlined in Table 1 are in agreement with the outcomes of test #1, indicating higher levels of photodegradation for CECs with higher ε_{254nm} (>10^4 M^{-1} cm^{-1}, DRN, IOP, LSTN, and SMX) and/or Φ_{254nm} (>10^{-1} mol E^{-1}, as for DCF). The low photolysis observed for other CECs (such as BSPL, ISTN, and VLX) was anticipated due to the presence of refractory organic functional groups, such as ether oxide bond (-*O*-), chloride (-Cl), and imine (-CH═N-) (Verlicchi et al., 2023).

While MSE post-treatment with UV-C is already applied in some full-scale WWTPs (domestic and industrial), these results underscore the need to enhance UV-C photolysis to ensure effective degradation of recalcitrant compounds and consequent safer discharge or reuse. This is particularly relevant for CECs identified in the EU-UWWTD proposal, like CBZ, ISTN, and VLX, and for which UV-C photolysis was insufficient to ensure compliance with the envisaged treatment efficiency requirement.

3.1.3. Removal of CECs by UV-C/H_2O_2 and UV-C/chlorine

Compared to UV-C photolysis, the addition of H_2O_2 (continuous dosage of 5, 10, and 20 mg L^{-1}, tests #4 to #6, respectively) led to considerable improvements in removing several CECs (Fig. 2a). The average degradation considering all the 14 target CECs was 64%, 74%, and 61% for increasing H_2O_2 dose. Beyond the efficient removal (>80%) for the six target CECs highly susceptible to UV-C photolysis (i.e., CBS-EPX, DCF, DRN, IOP, LSTN, and SMX), average removals >60% were achieved for both β-blockers (ATNL and BSPL), CBZ, DEET, ISTN, VSTN, and VLX. This enhancement indicates that, besides direct UV-C photolysis of the target CECs, indirect oxidation occurred by $HO^{\bullet}$ radical generated from the photodecomposition of H_2O_2. The $HO^{\bullet}$ is a reactive electrophile, thus rapidly attacking the most electron-rich sites in the organic contaminants' molecules. The dominant degradation pathway involves H-abstraction (at either C-ring or C-substituent atom) and subsequent hydroxylation (Cvetnic et al., 2020). Furthermore, single electron transfer and radical addition, the other two main pathways in $HO^{\bullet}$ driven reactions, may also occur. Therefore, during HO• attack of the target CECs, the main degradation pathways involved will be the hydroxylation on the aromatic ring or the oxidation of functional groups (e.g., secondary amine for β-blocker agents (Kovács et al., 2022), amide group for CBZ (Xiao et al., 2020), carboxyl for DCF (Huang et al., 2020), amino group for IOP (Zhao et al., 2019), and sulfonamide for SMX (Yang et al., 2017)). Consequently, all target CECs present high kinetic constants for the reaction with $HO^{\bullet}$ ($k_{HO\bullet} \geq 10^9$), except for MLN ($k_{HO\bullet} \sim 10^4$) (see Table 1 for details). This agrees with the results obtained, as the only CEC that remained without signs of degradation was MLN. Indeed, MLN's unique resistance aligns with research findings by Maurino et al. (2016), suggesting that its oxidation by HO• is unfeasible. Instead, MLN's oxidation likely initiates with the formation of a radical cation through direct electron abstraction, a mechanism commonly observed in photocatalytic processes involving TiO_2 photo-generated holes.

On the other hand, UV-C/Chlorine treatments (continuous dosage of 5, 10, and 20 mg L^{-1}, tests #7 to #9, respectively) displayed limited action on the oxidation of CECs compared to H_2O_2 (Fig. 2b), despite the considerably higher oxidant consumption measured for the treatment tests (discussed below, Figure SM-2). Compared to UV-C photolysis, the UV-C/Chlorine treatments exhibited overall better performance, with particular relevance for BSPL (18% ± 1%), VSTN (17% ± 4%), and VLX (22% ± 4%), despite four CECs (ATNL, CBZ, DEET, and MLN) remaining with no signs of degradation. UV-C/Chlorine process produces two primary radicals, $HO^{\bullet}$ and $Cl^{\bullet}$, and may also generate secondary RCS, such as $Cl_2^{\bullet-}$ and $ClO^{\bullet}$. $Cl^{\bullet}$ with a standard redox potential of +2.4 V reacts with electron-rich moieties through one-electron oxidation, H-abstraction, and addition to unsaturated C–C bonds (Wu et al., 2017). Mechanistic studies by Minakata et al. (2017) suggest that H-abstraction and Chlorine adduct formation are the dominant pathways for $Cl^{\bullet}$ reaction with CECs. $Cl_2^{\bullet}$ is another strong oxidant with a standard potential of +2.0 V. It is selective for olefinic compounds and aromatics when the ring is substituted with hydroxyl, methoxy, and amino groups (Wu et al., 2017). $Cl_2^{\bullet}$ reacts via H-abstraction for aliphatic compounds, addition for olefins, and single electron transfer for aromatics bearing electron-donating groups (Wu et al., 2017). $ClO^{\bullet}$ with a standard potential of +1.5–1.8 V reacts rapidly with aromatics substituted with methoxy groups. Values for $k_{ClO\bullet} > 10^8\ M^{-1}s^{-1}$ indicate CECs containing electro-donating functional groups, such as CBZ, DCF, and SMX (Guo et al., 2019). These diverse reactive species coexisting in UV-C/Chlorine treatments may complement one other and contribute to CEC degradation. Not surprisingly, many authors report a superior performance of UV-C/Chlorine over UV-C/H_2O_2 for removing microcontaminants. However, this is not always evident in secondary wastewater matrices (Cerreta et al., 2019; Li et al., 2017; Wang et al., 2019).

In the present study, various factors may have collectively contributed to the lower performance of UV-C/Chlorine over UV-C/H_2O_2 treatment. The potential advantages of $HOCl/OCl^-$, including greater molar absorptivity and quantum yield, may have been shadowed by the lower molar dosage of free chlorine applied (~50% less) compared to H_2O_2. Furthermore, when dosed at 20 mg L^{-1} in the dark (test #3), around 58% of free chlorine was consumed, indicating a high affinity of chlorine to quickly react with the organic matter of the MSE. Consequently, when under UV-C irradiation, it is possible that a significant portion of chlorine is unavailable to contribute to the generation of reactive species and, therefore, to CEC degradation. This likely accounts for the near-complete consumption of free chlorine (up to 98%) when 20 mg L^{-1} of chlorine was dosed under UV-C radiation (test #9). The pH conditions during treatment also play a crucial role, especially in the UV-C/Chlorine process, where the dissociation of $HOCl/OCl^-$ (Reaction 1) affects the chlorine photolysis and radical formation (Khajouei et al., 2022). In our study, MSE presented a pH value of 7.7, with minor variations at the end of the UV-C/H_2O_2 and UV-C/Chlorine tests (7.7 ± 0.2 and 7.9 ± 0.1, respectively, Table SM-4). For pH > 7.5, significant implications arise in radical formation and scavenging kinetics within the UV-C/Chlorine process. As pH increases, not only does the formation of primary radical $HO^{\bullet}$ and $Cl^{\bullet}$ decrease (Reaction 2), but also $HO^{\bullet}$ radical scavenging becomes more significant since OCl^- is much more reactive than either HOCl (Reaction 4) or H_2O_2 (k_{H2O2} = 2.7 ×10^7 M^{-1} s^{-1}), making UV/Chlorine less competitive (Remucal and Manley, 2016). The scavenging effect also generates the secondary radical $ClO^{\bullet}$ (Reactions 4 and 5), which generally shows lower reactivity towards the target CECs than $Cl^{\bullet}$ (Table 1). Additionally, the presence of bicarbonate ions (HCO_3^-, pKa = 6.38) in MSE, with preferential reactions towards $Cl^{\bullet}$ (Reactions 6 to 8), may further decrease the contribution of $Cl^{\bullet}$ for CECs abatement in the UV-C/Chlorine treatments. The inhibitory effects of natural organic matter (NOM) could also influence the observed results, as NOM reactivities indicate a higher scavenging effect on $ClO^{\bullet}$ (k = 4.5 × 10^4 (mg L^{-1})$^{-1}$ s^{-1}) than on $HO^{\bullet}$ (k = 2.5 × 10^4 (mg L^{-1})$^{-1}$ s^{-1}) and $Cl^{\bullet}$ (k = 1.3 × 10^4 (mg L^{-1})$^{-1}$ s^{-1}).

$$HOCl \leftrightarrow H^+ + OCl^- \ (pKa = 7.5, \text{at } 25^{\circ}C) \quad (R1)$$

$$HOCl + h\nu \rightarrow HO^{\bullet} + Cl^{\bullet} \ (\Phi_{254nm} = 1.0\ M^{-1}E^{-1}) \quad (R2)$$

$$OCl^- + h\nu \rightarrow O^{\bullet-} + Cl^{\bullet} \left(\Phi_{254nm} = 0.6\ M^{-1}\ E^{-1}\right) \quad (R3)$$

$$HOCl/OCl^- + HO^{\bullet} \rightarrow ClO^{\bullet} + H_2O\ k_{HOCl} = 5 \times 10^8\ M^{-1}\ s^{-1}, k_{OCl-} = 8.8 \times 10^9\ M^{-1}\ s^{-1} \quad (R4)$$

$$HOCl/OCl^- + Cl^{\bullet} \rightarrow ClO^{\bullet} + Cl^- + H^+ k_{HOCl} = 3 \times 10^9\ M^{-1}\ s^{-1}, k_{OCl-} = 8.2 \times 10^9\ M^{-1}\ s^{-1} \quad (R5)$$

$$HCO_3^- + Cl^{\bullet} \rightarrow CO_3^{\bullet-} + H^+ + Cl^- k = 2.2 \times 10^8\ M^{-1}\ s^{-1} \quad (R6)$$

$$HCO_3^- + Cl_2^{\bullet-} \rightarrow CO_3^{\bullet-} + H^+ + 2Cl^- k = 8.0 \times 10^7\ M^{-1}\ s^{-1} \quad (R7)$$

$$HCO_3^- + HO^{\bullet} \rightarrow CO_3^{\bullet-} + H_2O\ k = 8.5 \times 10^6\ M^{-1}\ s^{-1} \quad (R8)$$

Considering prior results employing this same tube-in-tube photoreactor for MSE post-treatment, also spiked with several CECs, 10 μg L^{-1} each (with 11 CECs in common with the present study), some relevant observations for discussion follow. For photo-Fenton (PF) under neutral pH conditions (Santos et al., 2023), MSE post-treatment resulted in degradations >60% for CBZ-EPX, DCF, DRN, and LSTN, with a treatment time of 73.2 s, a catalyst dose of 5 Fe^{2+} mg L^{-1} and 40 mg H_2O_2 L^{-1} (1.2 mM). In this case, the iron-catalyst (Fe^{2+}) solution was permeated through the membrane and the strong acidic nature of the Fe^{2+} stock solution (pH = 2) minimized iron precipitation in the thin film of liquid around the membrane, simultaneously promoting Fe^{2+} photo-regeneration. Under the same rationale, the strongly alkaline nature of the NaClO stock solution (pH = 11.8) likely impacted the performance of the UV-C/Chlorine process, promoting OCl^- as the main free chlorine species in the vicinity of the membrane. Santos et al. (2023) also proved that persulfate ($S_2O_8^{2-}$) was a valid oxidant alternative, promoting a photo-Fenton-like reaction when applied at the same equimolar dose, where removals >60% were attained for three additional CECs (ATNL, BSPL, and CBZ) and ~20% for MLN, demonstrating sulfate radicals ability to oxidize this highly recalcitrant compound. Another research demonstrated the successful use of the membrane as an O_3 contactor (Presumido et al., 2023), yielding removals >80% or concentrations below LQ for 10 of the 11 CECs in common with this work (again, MLN was not oxidized), applying a specific ozone dose of 1.17 g O_3 per g DOC and a retention time of just 5.8 s.

In a comprehensive view of treatment scenario 1, the average degradation for the 14 target CECs in MSE was 41% for UVC-photolysis (test #1), 74% for UV-C/H_2O_2 (10 mg L^{-1}, test #5), and 46% for UV-C/Chlorine (10 mg oxidant L^{-1}, test #8). These results agree with the decrease verified for the MSE absorbance at 254 nm, a recognized surrogate parameter for CEC degradation (Lee et al., 2021; Yu et al., 2015). In this case, 254 nm absorbance dropped by 10% after UV-C photolysis, 27% ± 2% on average after UV-C/H_2O_2, and 17% ± 1% on average after UV-C/Chlorine (Table SM-4). No mineralization occurred for any photo-treatment tests (average final DOC of 23.6 ± 0.4 and 23.7 ± 0.2 mg L^{-1}, for UV-C/H_2O_2 and UV-C/Chlorine tests, respectively, Table SM-4). Also, COD variation at the end of the treatments was <10% (average final COD of 72 ± 3 mg L^{-1}), primarily attributed to expectable analytical deviations. The results for UV-C/H_2O_2 tests #5 and #6, hold significant promise for ensuring compliance with the requirements for the target CECs included in the EU-UWWTD proposal (>80 % for DCF, and >60 % for CBZ, ISTN, and VLX).

3.1.4. Ecotoxicological assessment

Acute toxicity, before and after the application of advanced oxidation treatment, was evaluated using the bioluminescent bacteria *A. fischeri* as the test organism. Neither MSE nor MSE spiked with target CECs (10 μg L^{-1} each) were toxic to this organism. Likewise, MSE samples following post-treatment with UV-C/H_2O_2 and UV-C/Chlorine were not toxic to *A. fischeri*.

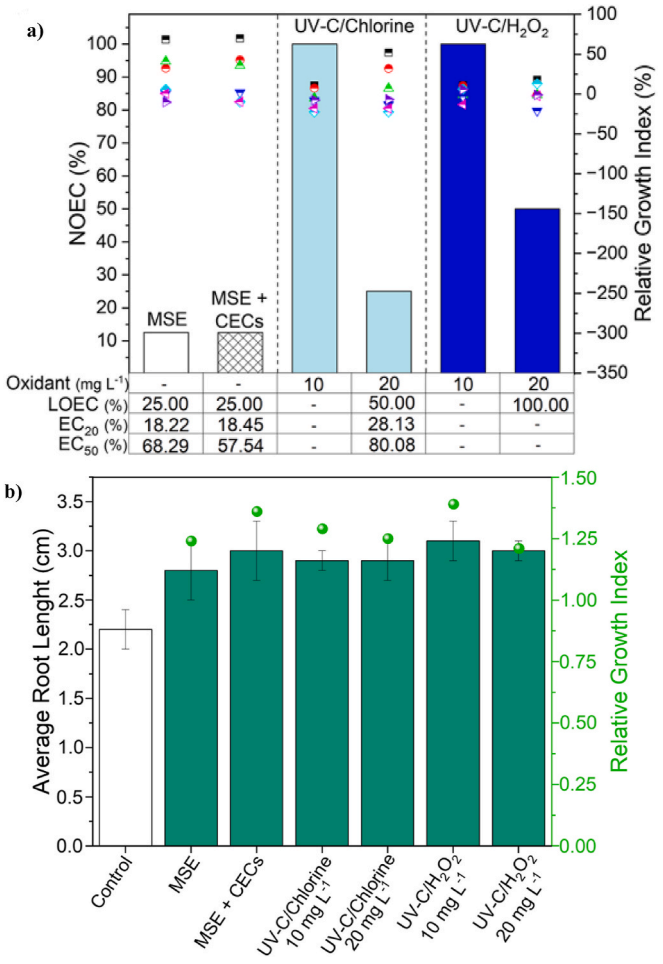

Fig. 3. a) Ecotoxicity to *Chlorella vulgaris* exposed to non-diluted MSE sample (■ 100%) and different dilution factors (DF): 50% (● DF 2), 25% (▲ DF 4), 12.5% (▼ DF 8), 6.25% (◆ DF 16), 3.12% (◀ DF 32), and 1.56% (▶ DF 64) (v/v), before and after UV-C/Chlorine (test #8 and #9) and UV-C/H_2O_2 (test #5 and #6) treatments. b) Phytotoxicity assessment with *Lactuca sativa* seeds from samples of MSE before and after UV-C/Chlorine and UV-C/H_2O_2. Note: MSE = municipal secondary effluent; MSE + CECs = municipal secondary effluent spiked with the 14 target CECs (10 μg L^{-1} each); NOEC = no observed effect concentration; LOEC = lowest observed effect concentration; EC_{50} = effective concentration for 50% of test organism; EC_{20} = effective concentration for 20% of test organism.

Chronic toxicity toward *Chlorella vulgaris* was also evaluated for MSE samples before and after applying the UV-AOPs. The results, depicted in Fig. 3a, revealed that MSE was toxic for *C. vulgaris*, showcasing a No Observed Effect Concentration (NOEC) equivalent to 12.5% (v/v) and an EC_{50} of 68.3%. This implies a dilution factor (DF) of 8 to eliminate sample toxicity to the test organism. Interestingly, the introduction of CECs into the MSE matrix did not influence toxicity toward this organism (NOEC = 12.5%; EC_{50} = 57.5%). A comparable pattern of ecotoxicity responses was observed for both applied UV-AOPs. For 10 mg L^{-1} of oxidant, test #5 (UV–C/H_2O_2) and test #8 (UV–C/Chlorine) completely removed toxicity to *C. vulgaris*. Notwithstanding, doubling the oxidant dose reduced initial toxicity to 75% for UV-C/H_2O_2 (test #6, with NOEC of 50% corresponding to DF = 2) and to 50% for UV-C/Chlorine (test #9, with NOEC of 25%, DF = 3, and an EC_{50} of 80.1).

Although treatment scenario 1 is being evaluated assuming final discharge into the environment, the possibility of reuse for applications that do not require reclaimed water quality class A cannot be ruled out. Phytotoxicity tests demonstrated that samples of MSE, before and after

UV-C/H_2O_2 and UV-C/Chlorine, were not toxic towards *Lactuca sativa* seeds (Fig. 3b). Experiments with initial concentrations of free chlorine and H_2O_2 at 10 and 20 mg L^{-1} stimulated root growth (relative growth index higher than 1.20), indicative of hormesis (Rodrigues-Silva et al., 2023).

3.2. Scenario 2: UV-AOP applied to nanofiltration retentate

3.2.1. Nanofiltration retentate

The NF_R applied in the photo-treatment tests for scenario 2 exhibited high levels of both organic and inorganic contamination, with COD value exceeding the legally stipulated limit for wastewater discharge into water compartments. Among the 14 target CECs, 11 were detected in the NF_R matrix, with ATNL (β-blocker agent), DEET (insect repellent), and VSTN (angiotensin II receptor blocker) registering concentrations < LQ (Table SM-3). Conversely, DCF (anti-inflammatory), IOP (X-ray contrast agent), and MLN (flame retardant) presented the highest concentrations (9.6, 12.3 and 21.2 μg L^{-1}, respectively). Since NF_R results from the concentration of MSE (although not from the MSE collected for scenario 1) and considering the expected negligible-to-low removals during secondary treatment, the concentrations of CECs observed in NF_R may surpass those in raw wastewater. This implies that for the NF_R treatment, a removal efficiency exceeding 80% for target CECs may be necessary to comply with the requirements anticipated by the EU-UWWTD proposal.

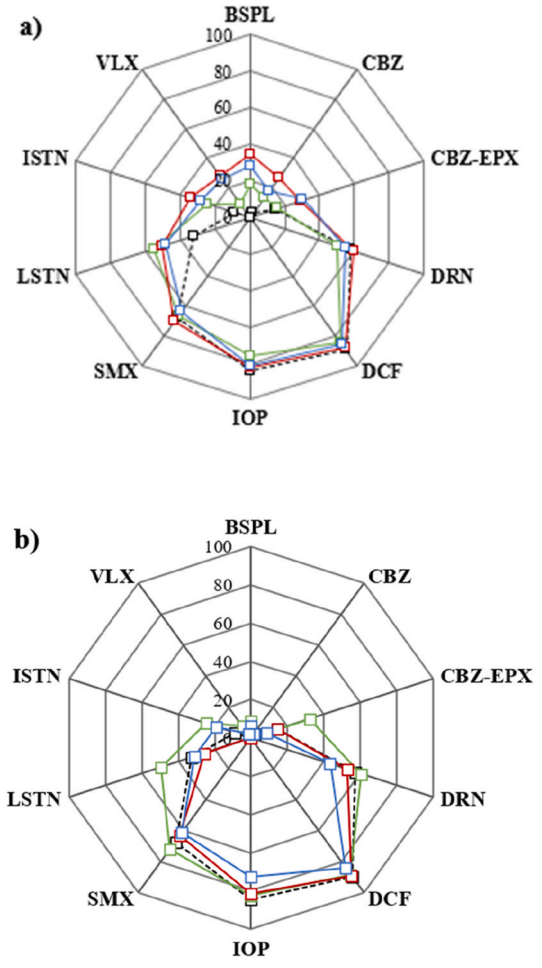

Fig. 4. Removal efficiencies (%) for the target CECs in NF_R for UV-C photolysis (-□- test #10) and UV-C/H_2O_2 or c) UV-C/NaHOCl. Oxidant dose of 20 mg L^{-1} (-□- tests #13 and #16), 40 mg L^{-1} (-□- tests #14 and #17) and 80 mg L^{-1} (-□- tests #15 and #18).

3.2.2. Removal of CECs by UV-C photolysis

Applying the UV-C process to the NF_R (test #10) demonstrated, once again, high efficiency in removing CECs more susceptible to photolysis. Substantial removal percentages were observed for DCF (90% ± 4%), IOP (84% ± 4%), DRN (58% ± 5%), and SMX (67% ± 4%). While to a lesser extent than observed in the MSE, some level of degradation was also achieved for the compounds CBZ-EPX (~15%) and LSTN (~33%). The remaining five CECs showed no evidence of removal.

The factors influencing light penetration and scattering effects, such as TSS content and turbidity, presented similar values between the wastewater matrices tested in this work (Table 2). Therefore, the lower performance demonstrated in UV-C photolysis when applied to NF_R may be primarily attributed to the higher content of aromatic organic compounds inherent in this matrix compared to MSE. This is substantiated by the specific ultraviolet absorbance at 254 nm ($SUVA_{254}$) of 1.0 L mg^{-1} m^{-1} for MSE (Table SM-4) and 2.3 L mg^{-1} m^{-1} for NF_R (Table SM-5), calculated as the ratio between UV-C absorbance at 254 nm (cm^{-1}) and the concentration of dissolved organic carbon (DOC, mg L^{-1}). A higher $SUVA_{254}$ value implies increased competition for UV-C photons during the photolysis process, resulting in fewer photons available to degrade the target CECs.

3.2.3. Removal of CECs by UV-C/H_2O_2 and UV-C/chlorine

In the absence of UV-C irradiation, the dosage of 80 mg H_2O_2 L^{-1} (test #11) led to an average decrease of 19% ± 3% for DCF, ISTN, and SMX (Figure SM-3); the remaining CECs had negligible removals (<10%). In the presence of UV-C, the continuous addition of 20, 40, and 80 mg H_2O_2 L^{-1} (tests #13 to #15, respectively) resulted in overall removals of 38%, 46%, and 43%, considering all the 11 target CECs detected in the NF_R. For the four CECs (BSPL, CBZ, ISTN, and VLX) that had no signs of degradation by UV-C alone, removals between 25% and 35% were observed, while CBZ-EPX and LSTN exhibited 2 times higher removals (Fig. 4a). In turn, for the UV-C/Chlorine tests (#16 to #18), no performance improvements were noted in the removal of the 11 target CECs when compared with UV-C alone (Fig. 4b). As observed for MSE, free chlorine was almost completely consumed at the end of the phototreatment tests, while H_2O_2 was not (Figure SM-4). This can be partially attributed to the combined effect of lower molar concentration applied in the treatment tests and the higher photolytic cleavage expected for HClO/ClO^- compared to H_2O_2 (as mentioned previously). Furthermore, reflecting the high reactivity of the oxidant to the NF_R components, free chlorine was highly consumed in dark conditions (67%, test #12), implying that higher chlorine dosages may be required for UV-C/Chlorine to be effective. In contrast, the high values of residual H_2O_2 still found at the end of the phototreatment tests suggest that a longer treatment time or a greater photonic flux could be applied and, thus, improve the performance in removing CECs. Like MSE, the only target CEC with abatements <10% for all tested conditions was MLN.

The lower efficiency of both tested UV-C/AOPs for NF_R compared to the tests carried out with MSE was anticipated, given the inherent complexity of the NF_R matrix underlined by the levels of in-/organic contamination (Table 2). As discussed for MSE, the pH value of NF_R (8.1) is expected to impair the generation of $HO^\bullet$ and $Cl^\bullet$ in UV-C/Chlorine (Reaction 2) and increase $HO^\bullet$ scavenging while producing the less reactive radical $ClO^\bullet$ (Reaction 4). Furthermore, the concentrations of Cl^- and SO_4^{2-} in NF_R are 4- and 10 times, respectively, higher than in MSE and can severely affect process efficiency by scavenging $HO^\bullet$ (Reactions 9 and 10) and $Cl^\bullet$ (Reaction 11).

$$Cl^- + HO^\bullet \rightarrow HOCl^{\bullet-} \quad k = 4.3 \times 10^9\ M^{-1}\ s^{-1} \tag{R9}$$

$$SO_4^{2-} + HO^\bullet \rightarrow SO_4^{\bullet-} + OH^- \ k = 2.7 \times 10^8\ M^{-1}\ s^{-1} \tag{R10}$$

$$Cl^- + Cl^\bullet \leftrightarrow Cl_2^{\bullet-} \ k = 6.5 \times 10^9\ M^{-1}\ s^{-1} \tag{R11}$$

As for MSE, no mineralization occurred for any of the photo-

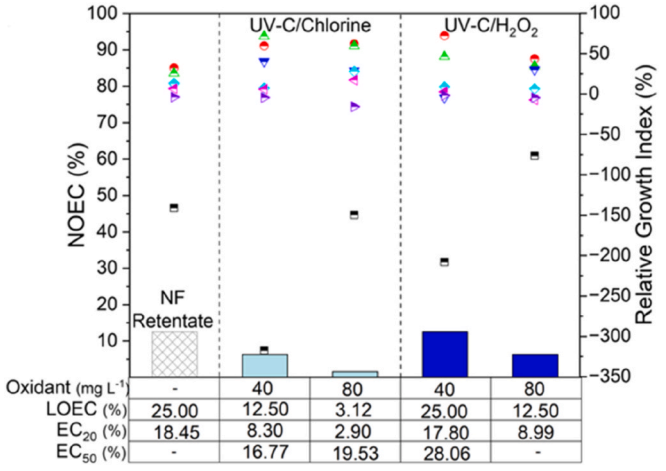

Fig. 5. Toxicity to *Chlorella vulgaris* exposed to non-diluted NF_R sample (■ 100%) and different dilution factors (DF; OECD culture medium): 50% (● DF 2), 25% (▲ DF 4), 12.5% (▼ DF 8), 6.25% (◆ DF 16), 3.12% (◀ DF 32), and 1.56% (▶ DF 64) (v/v), before and after UV-C/Chlorine (Test #17 and #18) and UV-C/H_2O_2 (Test #14 and #15) treatments. Note: NOEC = no observed effect concentration; LOEC = lowest observed effect concentration; EC_{50} = effective concentration for 50% of test organism; EC_{20} = effective concentration for 20% of test organism.

treatments, with average final DOC of 52 ± 1 and 51.4 ± 0.6 mg L^{-1}, for UV-C/H_2O_2 and UV-C/Chlorine tests, respectively. The decrease in NF_R absorbance at 254 nm was very limited and slightly above 10% only for UV-C/H_2O_2 treatments (Table SM-5). In contrast, COD decreased up to 122 and 135 mg L^{-1} (41% and 35% drop) at the end of the UV-C/H_2O_2 and UV-C/Chlorine with 40 mg of oxidant L^{-1} (tests #14 and #17, respectively, Table SM-5). This means that test #14 achieved a COD value below the legal limit for discharge into water compartments (<125 mg L^{-1}). COD reductions of 21%, 27%, and 30% were also observed for the tests with UV-C only (test #10) and H_2O_2 and NaClO oxidation under dark conditions (tests #11 and #12). This indicates that NF_R presents complex organic molecules that can be easily broken down into simpler and less oxidizable forms. The substantial reductions in COD observed after the UV-C/AOPs tests may be reflected in an increase in the biodegradability of the NF_R (not evaluated in this work), potentially making it more suitable for reintroduction back into the WWTP secondary treatment.

3.2.4. Ecotoxicological assessment

Before photo-treatment, NF_R exhibited NOEC and EC_{20} values for *C. vulgaris* of 12.5% and 18.5%, respectively (Fig. 5). These toxicity levels are similar to those observed for MSE before AOP treatment despite differences in the composition of each matrix (Table 2). However, unlike MSE, none of the proposed AOPs eliminated the chronic toxicity of NF_R towards *C. vulgaris*. In fact, the UV-C/Chlorine treatment increased toxicity, resulting in NOEC values of 6.3% (DF 16) and 1.6% (DF 64) with free chlorine concentrations at 40 and 80 mg L^{-1}, respectively. The complexity of this matrix, comprising NOM, inorganic species, and CECs, could give rise to toxic by-products, often referred to as disinfection by-products (DBPs) during these treatments (Young et al., 2018; Zhang et al., 2019). Some studies on secondary effluents have demonstrated that toxic DBPs, such as trichloromethane (THMs), haloacetic acids (HAAs), and nitrogenous DPBs, are formed during UV/Chlorine treatment and are correlated to the concentration of chlorine-based radicals generated in the system (Chen et al., 2023; Hua et al., 2021). This correlation could potentially explain toxicity observed for *C. vulgaris* in this study, as treatment of NF_R via UV-C/H_2O_2 (40 mg L^{-1}) did not increase sample toxicity, maintaining the NOEC at 12.5%.

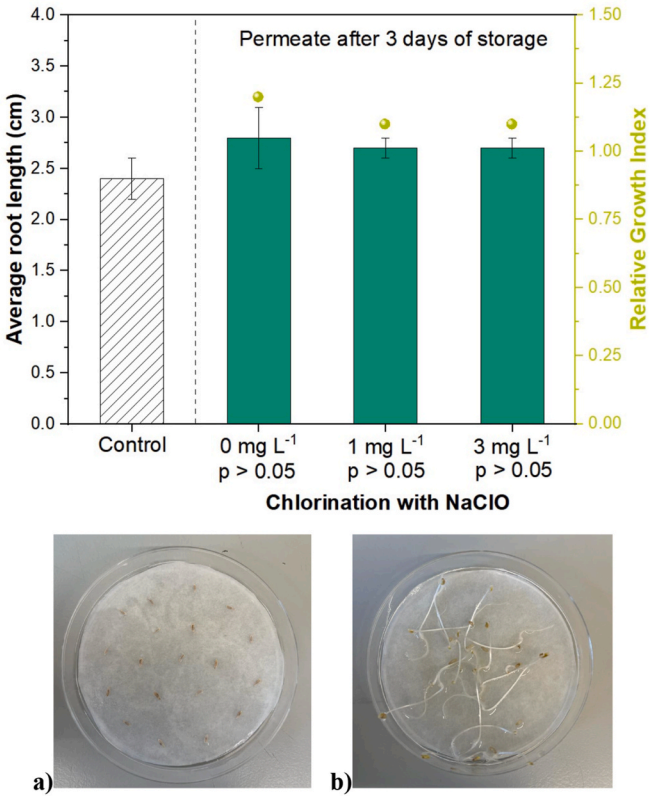

Fig. 6. Phytotoxicity assessment with *Lactuca sativa* seeds from samples of NF_P without and with disinfection by chlorine. Representative photographs of a) starting and b) end of phytotoxicity tests.

3.2.5. Potential reuse of nanofiltration permeate

In scenario 2, the NF_P produced from MSE presents high physicochemical quality, with very low in-/organic content, including the target CECs, with only MLN being detected (Table 2). From the 14 target CECs, MLN exhibits the lowest molecular weight, remaining below the NF membrane cutoff point (200–250 Da) and, therefore, was still found in the NF_P. The concentration of *E. coli* in this matrix was below 1 CFU 100 mL^{-1}, meeting the requirements for reclaimed water quality class A (≤10 CFU 100 mL^{-1}, (EURegulation_2020/741, 2020)). The high removal of *E.coli*, including those resistant to antibiotics, by NF of secondary effluents from WWTPs has been shown in other works (Schwermer et al., 2018). However, compliance with this requirement must be ensured up to the irrigation site and undesirable regrowth of bacteria through the reclaimed water distribution network may be anticipated. In this sense, the regrowth of *E. coli* in the NF_P matrix was evaluated after 3 days of storage, without disinfectant (test #19) and with the prior addition of two doses of free chlorine (1 and 3 mg L^{-1}, tests #20 and #21). Results show that only the test without NaClO addition registered *E. coli* regrowth (76 CFU 100 mL^{-1}), while the tests with disinfectant maintained *E. coli* levels <1 CFU 100 mL^{-1}. Residual chlorine is a crucial feature when considering water reuse for crop irrigation, with concentrations below 1 mg L^{-1} recognized as safe for plants, while concentrations exceeding 5 mg L^{-1} can cause severe damage to most plants (USEPA, 2012). After the 3-day storage period, free chlorine concentrations decreased by 23% and 18%, ensuring final residual chlorine <1 mg L^{-1} for test #20. Additionally, samples of the NF_P after 3-day storage, regardless of the disinfectant dose, exhibited no toxicity toward *Lactuca sativa* seeds (Fig. 6).

3.3. Comparison of treatment scenarios

This section compares the effectiveness of continuous UV-C

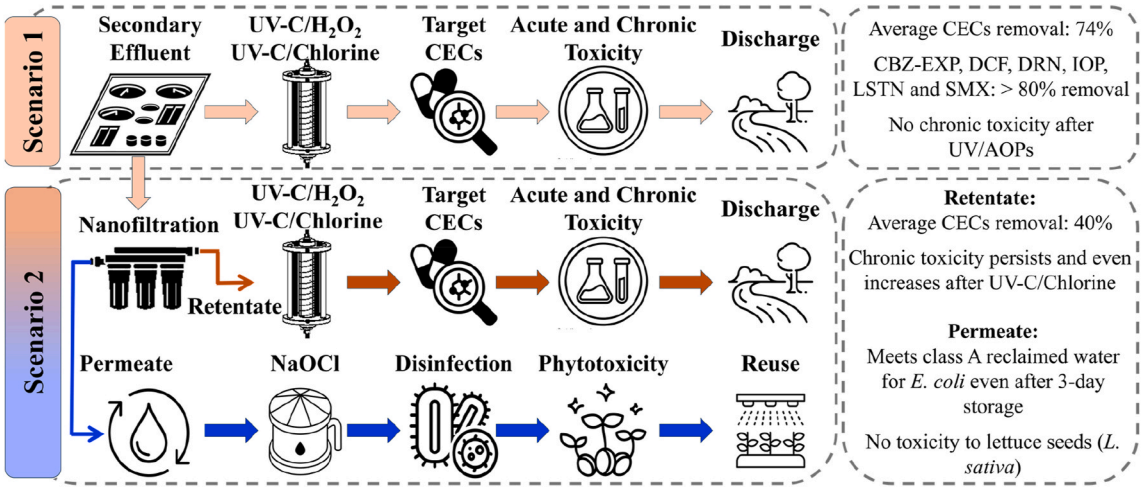

Fig. 7. Schematic representation of the treatment scenarios in this work.

photolysis, UV-C/H_2O_2, and UV-C/Chlorine in the wastewater treatment scenarios investigated in this work (Fig. 7). In scenario 1, MSE undergoes a UV-AOP stage before direct discharge into the environment. Despite meeting the physicochemical quality standards for discharge into water compartments, including COD and TSS as outlined in Directive 91/271/ECC and the EU-UWWTD proposal (Table 2), MSE still contains several CECs, including four target compounds specified in the upcoming EU-UWWTD (CBZ, DCF, ISTN, and VLX). This highlights the risk of non-compliance with future regulations and underscores the necessity of additional advanced treatment. In scenario 2, MSE undergoes nanofiltration, resulting in two streams: a retentate and a permeate. As expected, NF_R has higher levels of organic and inorganic contamination than MSE (Table 2) and fails to meet the COD threshold for discharge into the environment, indicating the need for further treatment even under current legislation. On the other hand, NF_P presents an opportunity for safe reuse in irrigation, aligning with the future EU-UWWTD's emphasis on promoting widespread water reclamation alongside new requirements for CECs abatement in WWTPs.

In both scenarios, the efficiency of the phototreatment stage was assessed by considering the removal of 14 CECs. In scenario 1, UV-C photolysis effectively degraded CECs readily susceptible to light, such as DCF, DRN, IOP, and SMX, but showed insufficient removal of other relevant CECs. While UV-C/Chlorine displayed limited performance, the UV-C/H_2O_2 achieved promising results, presenting the highest average removal efficiency (74%) for all CECs, with some exceeding 80%, a benchmark set by the proposed EU-UWWTD. In contrast, in scenario 2, all phototreatments resulted in lower efficiencies in removing CECs compared to scenario 1. The limited performance observed for the phototreatment stage can be attributed to the greater complexity of the NF_R matrix over MSE, characterized by a considerably higher content of organic and inorganic compounds (as pointed out above). Once again, UV-C/H_2O_2 treatment showed superior performance (average removal efficiency of 46%), highlighting its potential for advanced wastewater treatment.

Several factors influenced the effectiveness of each UV-driven AOP in both wastewater matrices. The slightly alkaline pH conditions (7.7 for MSE and 8.1 for NF_R) hindered treatment performance, especially for the UV-C/Chlorine process, affecting chlorine photolysis and radical formation. Additionally, the effectiveness of both UV/AOPs was impacted by the presence of natural organic matter, bicarbonate, chlorine, and sulfate ions, which likely acted as competitors or scavengers for radicals generated during treatment. This effect was more pronounced in scenario 2. It is worth noting that none of the UV-driven processes resulted in the mineralization of the MSE (scenario 1) or NF_R (scenario 2). Yet, a significant reduction in COD was observed for NF_R, potentially improving its biodegradability.

Beyond examining CEC removal, this study investigated the ecotoxicological effects of the treated wastewater in both Scenarios. Neither the raw MSE nor NF_R exhibited acute toxicity to *A. fischeri* before or after treatment; however, chronic toxicity towards *C. vulgaris* was observed before treatment in both matrices. This suggests that chronic toxicity tests may be more adequate for assessing the ecological safety of treated urban wastewater. Interestingly, before treatment, MSE and NF_R presented similar toxicity levels to *C. vulgaris* (NOEC of 12.5%). While chronic toxicity was eliminated after UV/AOP treatments in scenario 1, toxicity not only persisted after all phototreatments but increased after the UV-C/Chlorine process in scenario 2. The higher toxicity found for NF_R after the UV-C/Chlorine treatment may be attributed to the potential formation of DBPs, requiring further optimization for downstream discharge and investigation of the interaction between matrix compounds and chlorine reactions. Furthermore, in scenario 2, NF_P derived from MSE exhibited high quality, meeting reclaimed water class A standards for *E. coli* even after storage for 3 days with a single chlorine addition and no toxic endpoint to lettuce seeds (*L. sativa*).

4. Conclusions

The application of UV-C/H_2O_2 and UV-C/Chlorine processes, in continuous mode (residence time of 3.4 min) using a tubular membrane photoreactor, provided valuable insights into the removal efficiency of target CECs and the resulting ecotoxicity, considering two scenarios for municipal wastewater treatment. In scenario 1, MSE post-treatment with both UV-C/AOPs (3.3 kJ L^{-1} and 10 mg L^{-1} of H_2O_2 or Cl_2) resulted in complete removal of chronic toxicity to the microalgae *Chlorella vulgaris*, with UV-C/H_2O_2 outperforming in meeting future target CECs removal requirements in WWTPs. In scenario 2, the complexity of the NF_R matrix posed challenges, limiting the ability of both UV-C/AOPs to oxidize CECs. Moreover, none of the UV-C/AOPs could eliminate the chronic toxicity of NF_R to *C. vulgaris*, and UV-C/Chlorine even increased toxicity. Beyond this, the NF_P derived from MSE exhibited minimal CEC content and *E. coli* levels below regulatory limits for reuse in crop irrigation. Adding 1 mg Cl_2 L^{-1} effectively prevented *E. coli* regrowth during a 3-day storage period, ensuring compliance with reclaimed water quality standards and residual chlorine concentrations within safe limits for crop irrigation.

Despite the distinct treatment performances for the tested scenarios, common patterns emerged across both wastewater matrices. Certain CECs displayed high susceptibility to UV-C photolysis (namely for DCF, DRN, IOP, LSTN, and SMX) and UV-C/Chlorine consistently demonstrated lower efficiency in CECs removal compared to UV-C/H_2O_2. This

is attributed to the lower molar concentration of oxidant applied in the UV-C/Chlorine tests, coupled with the high reactivity of chlorine towards organic matter. The slightly basic pH of both matrices (7.7 for MSE and 8.1 for NF_R) and the strong alkaline character of the oxidant solution continuously delivered to the system (pH of 11.8), further hindered the oxidation capacity of the UV-C/Chlorine process in this work. These findings contribute to understanding the potential applications and limitations of UV-C/Chlorine and UV-C/H_2O_2 processes in distinct wastewater treatment scenarios, emphasizing the need for tailored approaches to safeguard water resources and mitigate the environmental impact of emerging contaminants. Moreover, this work points out future research efforts required to (i) explain the photochemical and oxidative processes involved in the degradation of target CECs, elucidating specific degradation pathways, (ii) characterize DBPs formed during the UV-C/Chlorine process, as inferred by toxicity levels in NF_R after treatment, along with the development of strategies to mitigate their formation, and (iii) evaluate the biodegradability of treated NF_R and its implications for reintroduction into WWTPs secondary treatment processes, offering potential new insights to deal with the challenges posed by this complex matrix.

CRediT authorship contribution statement

Fernando Rodrigues-Silva: Writing – original draft, Investigation, Formal analysis. **Carla S. Santos:** Writing – review & editing, Investigation. **Joaquín A. Marrero:** Writing – review & editing, Investigation. **Rosa Montes:** Writing – review & editing, Investigation. **José Benito Quintana:** Writing – review & editing, Resources. **Rosario Rodil:** Writing – review & editing, Resources. **Olga C. Nunes:** Writing – review & editing, Resources. **Maria Clara V.M. Starling:** Writing – review & editing, Supervision, Resources. **Camila C. Amorim:** Writing – review & editing, Supervision, Resources. **Ana I. Gomes:** Writing – original draft, Visualization, Supervision, Conceptualization. **Vítor J.P. Vilar:** Writing – review & editing, Supervision, Resources, Conceptualization.

Declaration of competing interest

The authors declare that they have no known competing financial interests or personal relationships that could have appeared to influence the work reported in this paper.

Data availability

No data was used for the research described in the article.

Acknowledgements

This work is financially supported by the program ERA-NET-European Research Area networks through national funds by Foundation for Science and Technology, I.P under the project SERPIC - Sustainable electrochemical reduction of contaminants of emerging concern and pathogens in WWTP effluent for irrigation of crops", with the reference Aquatic/0002/2020 (http://doi.org/10.54499/Aquatic/0002/2020). This work was also supported by national funds through FCT/MCTES (PIDDAC): LSRE-LCM, UIDB/50020/2020 (DOI: 10.54499/UIDB/50020/2020) and UIDP/50020/2020 (DOI: 10.54499/UIDP/50020/2020); and ALiCE, LA/P/0045/2020 (DOI: 10.54499/LA/P/0045/2020). Authors also want to acknowledge funding provided by Xunta de Galicia (ED431C 2021/06) and the Spanish Agencia Estatal de Investigación – MCIN/AEI/10.13039/501100011033 (ref. PID2021-117686RB-C32). Fernando Rodrigues-Silva acknowledges the CAPES – Brazilian international mobility scholarship under the CAPES-PRINT program (001; process n. 88887.695647/2022-00). Carla S. Santos acknowledges her PhD scholarship funded by FCT (2022.1079.BD). Vítor J.P. Vilar acknowledges the FCT Individual Call to Scientific Employment Stimulus 2017 (CEECIND/01317/2017).

Appendix A. Supplementary data

Supplementary data to this article can be found online at https://doi.org/10.1016/j.chemosphere.2024.142355.

References

91/271/EEC, D, 1991. In: Council Directive 91/271/EEC of 21st of May 1991 Concerning Urban Wastewater Treatment. Council, E.

Allard, S., Criquet, J., Prunier, A., Falantin, C., Person, A.L., Tang, J.Y.-M., Croué, J.-P., 2016. Photodecomposition of iodinated contrast media and subsequent formation of toxic iodinated moieties during final disinfection with chlorinated oxidants. Water Res. 103, 453–461. https://doi.org/10.1016/j.watres.2016.07.050.

APHA, 2017. Standard Methods for Examination of Water and Wastewater. American Public Health Association (APHA), American Water Works Association (AWWA) and Water Environment Federation (WEF).

Baeza, C., Knappe, D.R.U., 2011. Transformation kinetics of biochemically active compounds in low-pressure UV Photolysis and UV/H_2O_2 advanced oxidation processes. Water Res. 45 (15), 4531–4543. https://doi.org/10.1016/j.watres.2011.05.039.

Baxendale, J.H., Wilson, J.A., 1957. The photolysis of hydrogen peroxide at high light intensities. Trans. Faraday Soc. 53, 344–356. https://doi.org/10.1039/TF9575300344.

Bessa, V.S., Moreira, I.S., Van Loodrecht, M.C.M., Castro, P.M.L., 2021. Biological removal processes in aerobic granular sludge exposed to diclofenac. Environ. Technol. 3295–3308. https://doi.org/10.1080/09593330.2021.1921048.

Castellanos, R.M., Bassin, J.P., Dezotti, M., Boaventura, R.A.R., Vilar, V.J.P., 2020. Tube-in-tube membrane reactor for heterogeneous TiO2 photocatalysis with radial addition of H2O2. Chem. Eng. J. 395, 124998 https://doi.org/10.1016/j.cej.2020.124998.

Cerreta, G., Roccamante, M.A., Oller, I., Malato, S., Rizzo, L., 2019. Contaminants of emerging concern removal from real wastewater by UV/free chlorine process: a comparison with solar/free chlorine and UV/H_2O_2 at pilot scale. Chemosphere 236, 124354. https://doi.org/10.1016/j.chemosphere.2019.124354.

Chen, C., Zhao, X., Chen, H., Li, M., Cao, L., Wang, Y., Xian, Q., 2023. Degradation of natural organic matter and disinfection byproducts formation by solar photolysis of free available chlorine. Water Res. 239, 120020 https://doi.org/10.1016/j.watres.2023.120020.

Cvetnic, M., Tomic, A., Sigurnjak, M., Stankov, M.N., Ukic, S., Kusic, H., Bolanca, T., Bozic, A.L., 2020. Structural features of contaminants of emerging concern behind empirical parameters of mechanistic models describing their photooxidative degradation. J. Water Proc. Eng. 33, 101053 https://doi.org/10.1016/j.jwpe.2019.101053.

Díaz-Angulo, J., Cotillas, S., Gomes, A.I., Miranda, S.M., Mueses, M., Machuca-Martínez, F., Rodrigo, M.A., Boaventura, R.A.R., Vilar, V.J.P., 2021. A tube-in-tube membrane microreactor for tertiary treatment of urban wastewaters by photo-Fenton at neutral pH: a proof of concept. Chemosphere 263, 128049. https://doi.org/10.1016/j.chemosphere.2020.128049.

Diório, A., Díaz-Angulo, J., Castellanos, R.M., Gomes, A.I., Bergamasco, R., Vieira, M.F., Dezotti, M., Mueses, M., Machuca-Martínez, F., Vilar, V.J.P., 2021. A tubular ceramic membrane coated with TiO_2-P25 for radial addition of H_2O_2 towards AMX removal from synthetic solutions and secondary urban wastewater. Environ. Sci. Pollut. Control Ser. https://doi.org/10.1007/s11356-021-14297-4.

Espíndola, J.C., Vilar, V.J.P., 2020. Innovative light-driven chemical/catalytic reactors towards contaminants of emerging concern mitigation: a review. Chem. Eng. J. 394, 124865 https://doi.org/10.1016/j.cej.2020.124865.

EU-UWWTD, 2022. In: Proposal for a Directive of the European Parliament and of the Council Concerning Urban Wastewater Treatment. Commission, E.

EURegulation 2020/741, 2020. In: Regulation (EU) 2020/741 on Minimum Requirements for Water Reuse. Official Journal of the Eurpean Union. COUNCIL, E.P.A.O.T.

Farzanehsa, M., Vaughan, L.C., Zamyadi, A., Khan, S.J., 2023. Comparison of UV-Cl and UV-H_2O_2 advanced oxidation processes in the degradation of contaminants from water and wastewater: a review. Water Environ. J. 37 (4), 633–643. https://doi.org/10.1111/wej.12868.

Feng, Y., Smith, D.W., Bolton, J.R., 2007. Photolysis of aqueous free chlorine species (HOCl and OCl^-) with 254 nm ultraviolet light. J. Environ. Eng. Sci. 6 (3), 277–284. https://doi.org/10.1139/s06-052.

Guo, K., Wu, Z., Yan, S., Yao, B., Song, W., Hua, Z., Zhang, X., Kong, X., Li, X., Fang, J., 2018. Comparison of the UV/chlorine and UV/H_2O_2 processes in the degradation of PPCPs in simulated drinking water and wastewater: kinetics, radical mechanism and energy requirements. Water Res. 147, 184–194. https://doi.org/10.1016/j.watres.2018.08.048.

Guo, K., Wu, Z., Fang, J., 2019. Contaminants of Emerging Concern in Water and Wastewater: Advanced Treatment Processes. Elsevier.

Hua, Z., Li, D., Wu, Z., Wang, D., Cui, Y., Huang, X., Fang, J., An, T., 2021. DBP formation and toxicity alteration during UV/chlorine treatment of wastewater and the effects of ammonia and bromide. Water Res. 188, 116549 https://doi.org/10.1016/j.watres.2020.116549.

Huang, Y., Kong, M., Coffin, S., Cochran, K.H., Westerman, D.C., Schlenk, D., Richardson, S.D., Lei, L., Dionysiou, D.D., 2020. Degradation of contaminants of emerging concern by UV/H_2O_2 for water reuse: kinetics, mechanisms, and cytotoxicity analysis. Water Res. 174, 115587 https://doi.org/10.1016/j.watres.2020.115587.

Huber, M.M., Canonica, S., Park, G.-Y., von Gunten, U., 2003. Oxidation of pharmaceuticals during ozonation and advanced oxidation processes. Environ. Sci. Technol. 1 (5), 1016–1024. https://doi.org/10.1021/es025896h.

Ike, I.A., Karanfil, T., Cho, J., Hur, J., 2019. Oxidation byproducts from the degradation of dissolved organic matter by advanced oxidation processes – a critical review. Water Res. 164 https://doi.org/10.1016/j.watres.2019.114929.

ISO, 2007. Water Quality — Determination of the Inhibitory Effect of Water Samples on the Light Emission of Vibrio Fischeri (Luminescent Bacteria Test) — Part 3: Method Using Freeze-Dried Bacteria.

Kasonga, T.K., Coetzee, M.A.A., Kamika, I., Ngole-Jeme, V.M., Momba, M.N.B., 2021. Endocrine-disruptive chemicals as contaminants of emerging concern in wastewater and surface water: a review. J. Environ. Manag. 277, 111485 https://doi.org/10.1016/j.jenvman.2020.111485.

Khajouei, G., Finklea, H.O., Lin, L.-S., 2022. UV/chlorine advanced oxidation processes for degradation of contaminants in water and wastewater: a comprehensive review. J. Environ. Chem. Eng. 10 (3), 107508 https://doi.org/10.1016/j.jece.2022.107508.

Krzeminski, P., Tomei, M.C., Karaolia, P., Langenhoff, A., Almeida, C.M.R., Felis, E., Gritten, F., Andersen, H.R., Fernandes, T., Manaia, C.M., Rizzo, L., Fatta-Kassinos, D., 2019. Performance of secondary wastewater treatment methods for the removal of contaminants of emerging concern implicated in crop uptake and antibiotic resistance spread: a review. Sci. Total Environ. 648, 1052–1081. https://doi.org/10.1016/j.scitotenv.2018.08.130.

Lee, B.C.Y., Lim, F.Y., Loh, W.H., Ong, S.L., Hu, J., 2021. Emerging contaminants: an overview of recent trends for their treatment and management using light-driven processes. Water 13 (17), 2340. https://doi.org/10.3390/w13172340.

Lei, Y., Cheng, S., Luo, N., Yang, X., An, T., 2019. Rate constants and mechanisms of the reactions of $Cl^{\bullet}$ and $Cl_2^{\bullet-}$ with trace organic contaminants. Environ. Sci. Technol. 53 (19), 11170–11182. https://doi.org/10.1021/acs.est.9b02462.

Lei, Y., Westerhoff, P., Zhang, X., Yang, X., 2021. Reactivity of chlorine radicals ($Cl^{\bullet}$ and $Cl_2^{\bullet-}$) with dissolved organic matter and the formation of chlorinated byproducts. Environ. Sci. Technol. 55, 689–699. https://doi.org/10.1021/acs.est.0c05596.

Li, W., Jain, T., Ishida, K., Liu, H., 2017. A mechanistic understanding of the degradation of trace organic contaminants by UV/hydrogen peroxide, UV/persulfate and UV/free chlorine for water reuse. Environ. Sci. J. Integr. Environ. Res.: Water Research & Technology 3 (1), 128–138. https://doi.org/10.1039/C6EW00242K.

Lumbaque, E.C., Sirtori, C., Vilar, V.J.P., 2020. Heterogeneous photocatalytic degradation of pharmaceuticals in synthetic and real matrices using a tube-in-tubemembrane reactor with radial addition of H_2O_2. Sci. Total Environ. 743, 140629 https://doi.org/10.1016/j.scitotenv.2020.140629.

Lumbaque, E.C., Lüdke, D.S., Dionysiou, D.D., Vilar, V.J.P., 2021. Tube-in-tube membrane photoreactor as a new technology to boost sulfate radical advanced oxidation processes. Water Res. 191, 116815 https://doi.org/10.1016/j.watres.2021.116815.

Maurino, V., Minella, M., Sordello, F., Minero, C., 2016. A proof of the direct hole transfer in photocatalysis: the case of melamine. Appl. Catal. Gen. 521, 57–67. https://doi.org/10.1016/j.apcata.2015.11.012.

Minakata, D., Kamath, D., Maetzold, S., 2017. Mechanistic insight into the reactivity of chlorine-derived radicals in the aqueous-phase UV–chlorine advanced oxidation process: quantum mechanical calculations. Environ. Sci. Technol. 51, 6918–6926. https://doi.org/10.1021/acs.est.7b00507.

Miralles-Cuevas, S., Oller, I., Agüera, A., Sanchez-Peres, J.A., Sanchez-Moreno, R., Malato, S., 2016. Is the combination of nanofiltration membranes and AOPs for removing microcontaminants cost effective in real municipal wastewater effluents? Environ. Sci. J. Integr. Environ. Res.: Water Research & Technology 2, 511–520. https://doi.org/10.1039/C6EW00001K.

Montes, R., Méndez, S., Carro, N., Cobas, J., Alves, N., Neuparth, T., Santos, M.M., Quintana, J.B., Rodil, R., 2022. Screening of contaminants of emerging concern in surface water and wastewater effluents, assisted by the persistency-mobility-toxicity criteria. Molecules 27 (12), 3915. https://doi.org/10.3390/molecules27123915.

Nogueira, R.F.P., Oliveira, M.C., Paterlini, W.C., 2005. Simple and fast spectrophotometric determination of H_2O_2 in photo-Fenton reactions using metavanadate. Talanta 66, 86–91. https://doi.org/10.1016/j.talanta.2004.10.001.

OECD, 2011. Test No. 201: Freshwater alga and cyanobacteria, growth inhibition test. In: OECD Guidelines for the Testing of Chemicals.

Paxéus, N., 2004. Removal of selected non-steroidal anti-inflammatory drugs (NSAIDs), gemfibrozil, carbamazepine, beta-blockers, trimethoprim and triclosan in conventional wastewater treatment plants in five EU countries and their discharge to the aquatic environment. Water Sci. Technol. 50 (5), 253–260. https://pubmed.ncbi.nlm.nih.gov/15497855/.

Peres, J.C.G., Silvio, U., Teixeira, A.C.S.C., Guardani, R., Junior, A.D.V., 2015. Study of an annular photoreactor with tangential inlet and outlet: I. Fluid dynamics. Chem. Eng. Technol. 38 (2), 311–318.

Pistocchi, A., Alygizakis, N.A., Brack, W., Boxall, A., Cousins, I.T., Drewes, J.E., Finckh, S., Gallé, T., Launay, M.A., McLachlan, M.S., Petrovic, M., Schulze, T., Slobodnik, J., Ternes, T., Wezel, A., Verlicch, P., Whalley, C., 2022. European scale assessment of the potential of ozonation and activated carbon treatment to reduce micropollutant emissions with wastewater. Sci. Total Environ. 848, 157124 https://doi.org/10.1016/j.scitotenv.2022.157124.

Porto, B., Silva, T.F.C.V., Gonçalves, A.L., Esteves, A.F., de Souza, S.M.A.G.U., de Souza, A.A.U., Pires, J.C.M., Vilar, V.J.P., 2022. Tubular photobioreactors illuminated with LEDs to boost microalgal biomass production. Chem. Eng. J. 435, 134747 https://doi.org/10.1016/j.cej.2022.134747.

Presumido, P.H., Ribeirinho-Soares, S., Montes, R., Quintana, J.B., Rodil, R., Ribeiro, M., Neuparth, T., Santos, M.M., Feliciano, M., Nunes, O.C., Gomes, A.I., Vilar, V.J.P., 2023. Ozone membrane contactor for tertiary treatment of urban wastewater: chemical, microbial and toxicological assessment. Sci. Total Environ. 892, 164492 https://doi.org/10.1016/j.scitotenv.2023.164492.

Remucal, C.K., Manley, D., 2016. The efficacy of chlorine photolysis as an advanced oxidation process for drinking water treatment. Environ. Sci. J. Integr. Environ. Res.: Water Research & Technology 2, 565–579. https://doi.org/10.1039/C6EW00029K.

Rizzo, L., Gernjak, W., Krzeminski, P., Malato, S., McArdell, C.S., Sanchez-Peres, J.A., Schaar, H., Fatta-Kassinos, D., 2020. Best available technologies and treatment trains to address current challenges in urban wastewater reuse for irrigation of crops in EU countries. Sci. Total Environ. 710, 136312 https://doi.org/10.1016/j.scitotenv.2019.136312.

Rodrigues-Silva, F., Paini, G., Pucholobek, P., Imoski, R., Prola, T., Bastos, C., Regina, C., Algarte, W., Hermes, F., Liz, M.V., 2022. Removal of micropollutants by UASB reactor and post-treatment by Fenton and photo-Fenton: matrix effect and toxicity responses. Environ. Res. 212, 113396 https://doi.org/10.1016/j.envres.2022.113396.

Rodrigues-Silva, F., Starling, M.C.V.M., Rodrigues, D.A.S., Amorim, C.C., 2023. Sustainable treatment of municipal secondary effluent from UASB systems by solar photo-Fenton: CECs removal and toxicity control. J. Environ. Chem. Eng. 11, 110675 https://doi.org/10.1016/j.jece.2023.110675.

Sá, M.F.T., Castro, V., Gomes, A.I., Morais, D.F.S., Braga, R.V.P.S.S., Saraiva, I., Souza-Chaves, B.M., Park, M., Fernández-Fernández, V., Rodil, R., Montes, R., Quintana, J.B., Vilar, V.J.P., 2022. Tracking pollutants in a municipal sewage network impairing the operation of a wastewater treatment plant. Sci. Total Environ. 817, 152518 https://doi.org/10.1016/j.scitotenv.2021.152518.

Salgado, R., Pereira, V.J., Carvalho, G., Soeiro, R., Gaffney, V., Almeida, V.V.C., Ferreira, E., Benoliel, M.J., Ternes, T.A., Oehmen, A., Reis, M.A.M., Noronha, J.P., 2013. Photodegradation kinetics and transformation products of ketoprofen, diclofenac and atenolol in pure water and treated wastewater. J. Hazard Mater. 244–245, 516–527. https://doi.org/10.1016/j.jhazmat.2012.10.039.

Santos, C., Herraiz-Carboné, M., Lacasa, E., Sáez, C., Montes, R., Quintana, J.B., Rodil, R., Gomes, A.I., Vilar, V.J.P., 2023. Continuous-flow titration of low iron doses to promote photo-Fenton and photo-Fenton-like processes at neutral pH. Chem. Eng. J. 476, 14665 https://doi.org/10.1016/j.cej.2023.146655.

Schwermer, C.U., Krzeminski, P., Wennberg, A.C., Vogelsang, C., Uhl, W., 2018. Removal of antibiotic resistant E. coli in two Norwegian wastewater treatment plants and by nano- and ultra-filtration. processes Water Science & Technology 77 (4), 1115–1126. https://doi.org/10.2166/wst.2017.642.

Sengar, A., Vijayanandan, A., 2022. Human health and ecological risk assessment of 98 pharmaceuticals and personal care products (PPCPs) detected in Indian surface and wastewaters. Sci. Total Environ. 807, 150677 https://doi.org/10.1016/j.scitotenv.2021.150677.

Starling, M.C.V.M., Neto, R.P.M., Pires, G.F.F., Vilela, P.B., Amorim, C.C., 2021. Combat of antimicrobial resistance in municipal wastewater treatment plant effluent via solar advanced oxidation processes: achievements and perspectives. Sci. Total Environ. 786, 147448 https://doi.org/10.1016/j.scitotenv.2021.147448.

Sun, P., Lee, W.-N., Zhang, R., Huang, C.-H., 2016. Degradation of DEET and caffeine under UV/chlorine and simulated sunlight/chlorine conditions. Environ. Sci. Technol. 50, 13265–13273. https://doi.org/10.1021/acs.est.6b02287.

USEPA, 2012. N.R.M.R.L.-O.o.R.a.. In: Guidelines for Water Reuse. Development (Cincinnati, Ohio).

Vasseghian, Y., Hosseinzadeh, S., Khataee, A., Dragoi, E.-N., 2021. The concentration of persistent organic pollutants in water resources: a global systematic review, meta-analysis and probabilistic risk assessment. Sci. Total Environ. 796, 149000 https://doi.org/10.1016/j.scitotenv.2021.149000.

Vazquez, L., Gomes, L.M.M.T., Presumido, P.H., Rocca, D.G.D., Moreira, R.F.P.M., Dagnac, T., Llompart, M., Gomes, A.I., Vilar, V.J.P., 2023. Tubular membrane photoreactor for the tertiary treatment of urban wastewater towards antibiotics removal: application of different photocatalyst/oxidant combinations and ozonation. J. Environ. Chem. Eng. 11, 109766 https://doi.org/10.1016/j.jece.2023.109766.

Verlicchi, P., Grillini, V., Lacasa, E., Archer, E., Krzeminski, P., Gomes, A.I., Vilar, V.J.P., Rodrigo, M.A., Gäbler, J., Schäfer, L., 2023. Selection of indicator contaminants of emerging concern when reusing reclaimed water for irrigation — a proposed methodology. Sci. Total Environ. 873, 162359 https://doi.org/10.1016/j.scitotenv.2023.162359.

Vilar, V.J.P., Alfonse-Muniozguren, P., Monteiro, J.P., Lee, J., Miranda, S.M., Boaventura, R.A.R., 2020. Tube-in-tube membrane microreactor for photochemical UVC/H_2O_2 processes: a proof of concept. Chem. Eng. J. 379, 122341 https://doi.org/10.1016/j.cej.2019.122341.

Wang, C., Moore, N., Bircher, K., Andrews, S., Hofmann, R., 2019. Full-scale comparison of UV/H_2O_2 and UV/Cl_2 advanced oxidation: the degradation of micropollutant surrogates and the formation of disinfection byproducts. Water Res. 161, 448–458. https://doi.org/10.1016/j.watres.2019.06.033.

Wang, T., Dai, X., Zhang, T., Xin, C., Guo, Z., Wang, J., 2022. Formation and microbial composition of biofilms in drip irrigation system under three reclaimed water conditions. Water 14. https://doi.org/10.3390/w14081216.

Wols, B.A., Hofman-Caris, C.H.M., Harmsen, D.J.H., Beerendonk, E.F., 2013. Degradation of 40 selected pharmaceuticals by UV/H_2O_2. Water Res. 14 (15), 5876–5888. https://doi.org/10.1016/j.watres.2013.07.008.

Wols, B.A., Harmsen, D.J.H., Wanders-Dikj, J., Beerendonk, E.F., Hofman-Caris, C.H.M., 2015. Degradation of pharmaceuticals in UV (LP)/H_2O_2 reactors simulated by means of kinetic modeling and computational fluid dynamics (CFD). Water Res. 75, 11–24. https://doi.org/10.1016/j.watres.2015.02.014.

Wu, Z., Guo, K., Fang, J., Yang, X., Xiao, H., Hou, S., Kong, X., Shang, C., Yang, X., Meng, F., Chen, L., 2017. Factors affecting the roles of reactive species in the degradation of micropollutants by the UV/chlorine process. Water Res. 126, 351–360. https://doi.org/10.1016/j.watres.2017.09.028.

Xiao, R., Ma, J., Luo, Z., Zeng, W., Wei, Z., Spinney, R., Hu, W.-P., Dionysiou, D.D., 2020. Experimental and theoretical insight into hydroxyl and sulfate radicals-mediated degradation of carbamazepine. Environ. Pollut. 257, 113498 https://doi.org/10.1016/j.envpol.2019.113498.

Yang, Y., Lu, X., Jiang, J., Ma, J., Liu, G., Cao, Y., Liu, W., Li, J., Pang, S., Kong, X., Luo, C., 2017. Degradation of sulfamethoxazole by UV, UV/H_2O_2 and UV/persulfate (PDS): formation of oxidation products and effect of bicarbonate. Water Res. 118, 196–207. https://doi.org/10.1016/j.watres.2017.03.054.

Young, T.R., Li, W., Guo, A., Korshin, G.V., Dodd, M.C., 2018. Characterization of disinfection byproduct formation and associated changes to dissolved organic matter during solar photolysis of free available chlorine. Water Res. 146, 318–327. https://doi.org/10.1016/j.watres.2018.09.022.

Yu, H.-W., Anumol, T., Park, M., Pepper, I., Scheideler, J., Snyder, S.A., 2015. On-line sensor monitoring for chemical contaminant attenuation during UV/H_2O_2 advanced oxidation process. Water Res. 81, 250–260. https://doi.org/10.1016/j.watres.2015.05.064.

Zhang, X., Zhai, J., Zhong, Y., Yang, X., 2019. Degradation and DBP formations from pyrimidines and purines bases during sequential or simultaneous use of UV and chlorine. Water Res. 165, 115023 https://doi.org/10.1016/j.watres.2019.115023.

Zhao, X., Jiang, J., Pang, S., Guan, C., Li, J., Wang, Z., Ma, J., Luo, C., 2019. Degradation of iopamidol by three UV-based oxidation processes: kinetics, pathways, and formation of iodinated disinfection byproducts. Chemosphere 221, 270–277. https://doi.org/10.1016/j.chemosphere.2018.12.162.